Improvement of transdermal delivery of sumatriptan succinate using novel water emulsion patch or self-dissolving microneedle array, and their *in vitro* and *in vivo* characterizations

Dan WU

Department of Biopharmaceutics,

Kyoto Pharmaceutical University

2014

TABLE OF CONTENTS

ABBREVIATIONS……1

ABSTRACT……...2

INTRODUCTION……6

CHAPTER 1 DEVELOPMENT OF A TRANSDERMAL WATER EMULSION PATCH SYSTEM INCORPORATING SS……10

1.1. Materials……..11

1.2. Fabrication of SS-incorporated patches……...11

1.3. Determination of SS contents in SS-incorporated patches……13

1.4. Measurement of adhesion properties of SS-incorporated patches……14

1.5. *In vitro* transdermal permeation of SS from SS-incorporated patches……15

1.6. Assessment of rat skin barrier disruption after application of SS-incorporated patches via TEWL values…….……..……...……...……...……...……...18

1.7. *In vivo* transdermal absorption of SS from SS-incorporated patches……...20

1.8. Discussion……24

CHAPTER 2 DEVELOPMENT OF A NOVEL SELF-DISSOLVING MN LOADED WITH SS……..28

2.1. Materials……29

2.2. Fabrication of sodium hyaluronate MNs……..……29

2.3. Improvement of transdermal delivery of SS from SS-loaded MNs……...……31

2.4. Measurement of mechanical failure force and hygroscopy of SS-loaded MNs……36

2.5. Estimation of skin penetration capacity of SS-loaded MNs……..40

2.6. *In vitro* release of SS from SS-loaded MNs……41

2.7. Evaluation of dissolution of SS-loaded MNs following inserting into rat skin…...42

2.8. Assessment of skin barrier disruption after application of SS-loaded MNs via TEWL values……..……43

2.9. Skin primary irritation after application of SS-loaded MNs to rat……...……45

2.10. Recovery of micropores created by insertion of MNs into rat skin……...46

2.11. *In vivo* transdermal absorption of SS from SS-loaded MNs……48

2.12. Discussion……52

COMPARISONS BETWEEN WATER EMULSION PATCH AND SELF-DISSOLVING MN……58

CONCLUSIONS……59

ACKNOWLEDGMENTS……60

REFERENCES……61

PUBLISHED PAPERS……...70

ABBREVIATIONS

ANOVA	Analysis of variance
AUC	Area under the plasma concentration-time curve
BA	Bioavailability
C_{max}	Maximal plasma drug concentration
3 D	Three-dimensional
2 D	Two-dimensional
HGA	HGA 64: hydrophilic acrylic adhesive
HPLC	High performance liquid chromatography
5-HT	5-hydroxytryptamine
LD	Lauric acid diethanolamide
i.v.	Intravenous
MN(s)	Microneedles array(s)
Nikasol	Nikasol TS620: 2-propenoic acid, 2-ethylhexyl ester polymer with methyl 2-propenoate
OCT	Optimal coherence tomography
PBS	Phosphate buffered saline
P.I.I.	Primary Irritation Index
s.c.	Subcutaneous
SDS	Sodium dodecyl sulfate
S.E.	Standard error of the mean
SS	Sumatriptan succinate
TEWL	Transepidermal water loss
T_{max}	Time to maximal plasma drug concentration

ABSTRACT

Sumatriptan succinate (SS), a selective serotonin 5-hydroxytryptamine (5-HT) agonist at the 5-HT_{1B} and 5-HT_{1D} receptors, is the most frequently prescribed migraine therapy among a class of drugs known collectively as the triptans. SS has been commercialized for administration by oral, nasal spray and subcutaneous injection. Unfortunately, these formulations are associated with variety of limitations that can lead to patients' delay or avoid treatment. For example, the difficulty in taking an oral medication due to the nausea and vomiting that often accompany migraine, and the low bioavailability of oral and nasal spray (15% and 17%, respectively), as well as the skin site reactions and the reluctance of self-injection associated with subcutaneous injection. Therefore, in order to suppress those limitations while sustaining the therapeutic efficacy of SS, an alternative more effective SS delivery method is necessary for anti-migraine therapeutics. Transdermal drug delivery allows the permeation of drugs across the skin and enters into the systemic circulation, thus avoiding degradation by the gastrointestinal tract and hepatic first-pass metabolism. This delivery system is considered to be user-friendly, and is convenient administration. However, its application is limited to only a few hydrophobic low molecular compounds because of the outermost skin barrier layer, stratum corneum. In particular, SS has high hydrophilicity (log $P_{\mathrm{pH\ 7.4}} = -0.86$) and it is difficult to pass through the skin barrier.

Based on these observations, in this study, I attempted to investigate two types of methodologies to improve the transdermal delivery of SS, including SS-incorporated passive patch and SS-loaded microneedle array (MN). An acrylic polymer emulsion, pressure sensitive adhesive Nikasol was chosen to prepare the SS-incorporated patch, and compared with a hydrophilic acrylic adhesive HGA. On the other hand, a novel self-dissolving MN was fabricated by employing sodium hyaluronate as the basic material. Various parameters such as needle lengths, thickness, and density as well as penetration enhancers were evaluated to

enhance *in vitro* skin permeation of SS from MNs. Furthermore, the *in vivo* efficacy of the SS-loaded MNs for transdermal delivery of SS was characterized.

1. Development of a transdermal water emulsion patch system incorporating SS

Two types of transdermal patches containing SS were prepared, using either water emulsion resin Nikasol (SS Nikasol patch) or hydrophilic acrylic adhesive HGA (SS HGA patch). The contents of SS in both formulations were 20% (w/w). The thickness of all patches used ranged from 40 to 45 μm. *In vitro* permeated studies showed that the permeability of SS from the Nikasol patch was greater than that of the HGA patch, making it an excellent candidate for the development of SS transdermal patches. It was also found that SS permeation from the Nikasol patch was lower in humans, as compared to rats. An increase in transepidermal water loss was observed after application of both types of patches, however, this parameter gradually recovered to baseline, suggesting that the skin barrier disruption was reversible. No visible irritation appeared after application of the transdermal patches to rat skin during the experimental period. Furthermore, *in vivo* pharmacokinetic studies indicated that the absorption of SS from Nikasol patch was significantly higher than that of the HGA patch, which was well consistent with the *in vitro* skin permeation results. In addition, SS was effectively absorbed from Nikasol patch through the skin and associated with relatively greater absolute bioavailability than that of oral administration, achieving a consistent plasma concentration over an extended period of time. These findings demonstrated that the novel patch system fabricated from emulsion Nikasol was a useful and promising alternative method to improve transdermal delivery of SS without any serious skin damage.

2. Development of a novel self-dissolving MN loaded with SS

SS-loaded MNs with different needle length, thickness, density and penetration enhancers were fabricated from sodium hyaluronate. All the needles were tapered cone-shaped in a

circular array with a diameter of 10 mm. MNs with the length of 800 μm could effectively improve the transdermal permeability of SS compared with that of 500 μm. No distinct enhancement was obtained by increasing the thickness of MNs or by adding penetration enhancers in the prescription of MNs. Further, skin permeability of SS could be significantly improved after increasing needle numbers. Therefore, high density MNs with needle length of 800 μm were chosen for the subsequent studies.

The resulting SS-loaded MNs possessed sufficient mechanical strength to successfully puncture the skin barrier and maintained their skin piercing abilities for at least 30 min after being placed at a high relative humidity of 75%. Optical coherence tomography images demonstrated that the MNs uniformly created drug permeation pathways after being inserted into the skin. Almost all of the formulated SS was released from the MNs at a relatively constant rate within 1 h via an *in vitro* release study. It was also noted that needles began to dissolve upon application onto rat skin *in vivo* and were completely dissolved within 1 h. These findings suggested that the novel MNs had biocompatible properties and SS appeared to be rapidly released from these MNs. Moreover, MNs significantly increased transepidermal water loss; however, skin barrier function gradually recovered to control levels within 24 h, in contrast to the skin damage observed after tape stripping treatment. These findings indicated that the micro-scale pathways created by the microneedles quickly resealed, and that the skin damage was reversible, which were highly consistent with the rapidly recovery of micropores created by insertion of blue dye contained MNs into rat skin. Furthermore, a dose-dependent plasma concentration of SS was obtained after treatment with SS-loaded MNs in rats. Pharmacokinetic characteristics indicated that absorption of SS delivered by MNs was similar to that observed after subcutaneous injection and was associated with high bioavailability (~90%), which was much higher than that produced by oral administration. These findings suggested that application of SS-loaded MNs to the skin provided an effective alternative approach to enhance the transdermal delivery of SS without serious skin damage, while

avoiding the pain caused by usage of hypodermic needles.

In conclusion, the present findings indicated that both the water emulsion patch choosing Nikasol as an adhesive and the self-dissolving MN fabricated from sodium hyaluronate were useful and promising alternative approaches to improve transdermal delivery of SS without serious skin damage. Further, the novel MN seems to be a much more effective method in clinical application due to the reasonable administration size and rapid onset of action, would be likely to improve patient compliance.

INTRODUCTION

Migraine is a chronic, intermittent neurologic disease characterized by episodes of headache and usually associated with nausea, vomiting, and sensitivity to light, sound and head movement; symptoms that typically last for 4-72 h [1,2]. The mainstay of acute migraine treatment is the so-called "triptans" Sumatriptan succinate (3-[2-(dimethylamino)ethyl]-*N*-methyl-1*H*-indol-5-methane-sulfonamide succinate, SS) (Fig. 1) is the first member of a class of drugs known collectively as triptans [3,4]. It is a selective serotonin 5-hydroxytryptamine (5-HT) agonist that activates the 5-HT_{1B} and 5-HT_{1D} receptors for the treatment of acute migraine attack. SS provides migraine relief by binding to 5-HT_1 receptors in the brain, resulting in the constriction of extracerebral blood vessels within the cranial vasculature and the inhibition of inflammatory mediator release from sensory nerve endings in the trigeminal system, thus preventing nociceptive transmission [5,6].

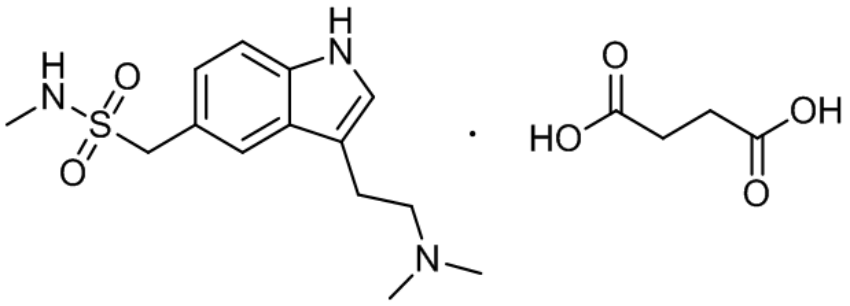

(Journal of Drug Delivery Science and Technology, Figure 1)

Fig. 1. Chemical structure of sumatriptan succinate (*MW* = 413.49 Da; p*K*a = 4.21, 5.67; log $P_{\text{pH 7.4}} = -0.86$).

SS has been commercialized for administration by oral, nasal spray and subcutaneous injection. Unfortunately, these formulations are associated with variety of limitations that can lead to patients' delay or avoid treatment [7]. Oral intake of SS is related to nausea and vomiting associated with a migraine episode. Furthermore, due to pre-systemic metabolism

and incomplete absorption, SS also has poor oral bioavailability (BA, 15%) [8-10]. Intranasal SS has low BA (17%), similar to oral SS, and can have a bitter taste and cause nose or throat discomfort [11]. Subcutaneous SS has a much higher BA (97%); however, injections sometimes associated with skin site reactions and atypical sensations, such as sensations of tingling, heat, pruritus or tightness, as well as the reluctance of self-injection [12]. Therefore, In order to suppress those limitations, an alternative more effective SS delivery method is necessary for anti-migraine therapeutics. Transdermal drug delivery allows drugs to permeate the skin and enter into systemic circulation, thus avoiding degradation by the gastrointestinal tract and hepatic first-pass metabolism. This delivery system is considered to be user-friendly, and is easily terminated [13,14]. However, its application is limited to only a few hydrophobic low molecular compounds because of the outermost layer of skin, stratum corneum. In particular, SS has high hydrophilicity (log $P_{\text{pH 7.4}} = -0.86$) and it is difficult to pass through the skin barrier [3,15,16]. Previous studies have involved a number of methods [16-20] to enhance the transdermal delivery of SS through the skin. Femenía-Font et al. [16] improved passive diffusion of SS through skin by combining it with a variety of chemical enhancers. Patel et al. [17] confirmed that significant amounts of SS could be delivered across the skin from solution formulations using an iontophoretic patch system. However, there are several disadvantages to such methods, including the large doses required, external devices, and adverse reactions at the application site.

Recent work has investigated the effect of adhesive factors on the *in vitro* and *in vivo* characteristics of candidate transdermal systems [21,22]. The choice and design of the pressure sensitive adhesive are critical, because it has a strong effect on the drug release and wear properties of the patch [23,24]. Nikasol TS620 (2-propenoic acid, 2-ethylhexyl ester polymer with methyl 2-propenoate, Nikasol), is an acrylic fiber system water emulsion resin. Nikasol has recently been shown to be a highly effective pressure sensitive adhesive in transdermal delivery system. Nikasol has several distinguishing characteristics that make it

suitable for use as an adhesive in the preparation of transdermal patch systems. First, Nikasol has high biocompatibility and physicochemical compatibility with many drugs, as well as other components of the system, such as penetration enhancers. This is important, as biocompatibility and physicochemical compatibility are primary consideration when choosing an adhesive. Further, Nikasol adhesion is lasting, which is necessary and important for long-term transdermal administration. Finally, Nikasol has a low risk of skin irritation, which improves the likelihood of patient compliance.

Based on these findings, we sought to develop a novel transdermal patch containing SS fabricated from Nikasol. Additionally, we assessed and compared the characteristics between Nikasol- and HGA-fabricated SS patches, because we previously reported the use of the hydrophilic acrylic adhesive HGA 64 in the development of a novel transdermal patch for the administration of alendronate, a nitrogen-containing bisphosphonate used in the treatment of osteoporosis [25]. The adhesion properties of the SS-incorporated patches were determined. *In vitro* skin permeation of SS from the patches was also examined. Moreover, disruption and irritation of skin after their application was assessed to confirm the safety of the patches. Further, *in vivo* transdermal absorption characteristics of SS from the patches were evaluated.

Although the patch system choosing Nikasol as an adhesive was feasible to improve the transdermal delivery of SS, the large patch size would be inconvenient in practical application. Therefore, another method to further improve the skin permeability of SS was necessary. In recent years, microneedle arrays (MNs) have received much attention as a novel, minimally invasive approach. These micron-sized needles disrupt the stratum corneum and create micro-scale pathways that can effectively increase transdermal transport of drugs [26-28]. These needles are long enough to breach the skin’s barrier to allow for drug transport, yet are short enough to avoid stimulating skin nerves, and therefore are painless in contrast to hypodermic needles [29,30]. MNs have been applied to the delivery of many types of compounds, ranging from low molecular weight drugs to proteins, plasmid DNA, as well as

the influenza virus [31-35]. In the previous researches, most MNs have been fabricated from silicon [34,36,37], metals [31,33,35,38,39] and glass [40]. However, these types of MNs are limited by their expensive material costs or an undesirable two-step administration process. In addition, choosing silicon, metals or glass as the basal material raises safety concerns, since MNs can be accidentally broken and may remain in the skin after application.

To overcome these shortcomings and limitations, MNs fabricated from biocompatible and biodegradable polymers [41-44] and water-soluble carbohydrates [45-49] have been developed recently. These MNs were completely degraded or dissolved in the skin interstitial fluid, thereby releasing their encapsulated drug; a one-step application. Nevertheless, the development of dissolving MN systems presents many obstacles. For example, fabrication of MNs at high temperatures can reduce the activities of their heat-sensitive cargoes, such as peptides and proteins [41,47,50]. In addition, carbohydrate-based MNs deformed readily under relatively humid conditions, which negatively affected the mechanical strength of the needles [46,47,51].

With these findings in mind, we used sodium hyaluronate to fabricate novel self-dissolving MNs in this study. Sodium hyaluronate is a water soluble polymer of disaccharides, naturally component of many tissues in the body, such as skin, cartilage and vitreous humor. It is used as a common ingredient in cosmetics. The high biocompatibility and other physiochemical properties of sodium hyaluronate make it suitable for preparation of the self-dissolving MNs. MNs were fabricated by micromolding technologies at room temperature. The effect of needle length, thickness, density and penetration enhancers on the skin permeability of SS from the MNs were assessed. Moreover, the properties of hygroscopy, skin penetration, dissolution and *in vitro* release of the SS-loaded MNs were investigated. The disruption, irritation and recovery of skin after their application were further evaluated to confirm the safety of these MNs. Furthermore, *in vivo* transdermal delivery of SS was evaluated and compared with subcutaneous (s.c.) injection or oral administration in rats.

CHAPTER 1 Development of a transdermal water emulsion patch system incorporating SS

SS is a drug with high hydrophilicity, and as such, SS does not easily pass through the stratum corneum barrier. I attempted to develop a novel transdermal patch fabricated from Nikasol, an acrylic fiber system water emulsion resin, to enhance the passive delivery of SS in sufficient therapeutic amounts. Importantly, the Nikasol-fabricated patch was simple in structure and did not require additional chemical enhancers or external devices to exert its effect on migraine.

For the SS-incorporated patches, an important problem is the appearance of crystallization. Crystallization can significantly reduce the release of drug from the patches. I tried to improve drug content, meanwhile, avoiding the generation of crystallization after long storage. It was found that SS could be incorporated up to 20% (w/w) without crystallization. Thus, an SS content of 20% was selected to give a similar driving force between the concentration gap and saturation concentration. Moreover, when the concentration of drug and other additives is same, a thicker adhesive layer is able to deliver higher amount of drug to the skin. The thickness of 40-45 μm was thus chosen to obtain relatively high cumulative skin permeability of SS. Additionally, our patches possessed good adhesive properties with the thickness.

In this study, the characteristics of Nikasol-fabricated patches were compared with a previously reported [25] hydrophilic acrylic adhesive HGA-fabricated patches. To determine the adhesion properties of the SS-incorporated patches, peel adhesion force and tackiness were measured. Furthermore, *in vitro* permeation of SS across human and rat skin was examined, and transepidermal water loss (TEWL) was determined to investigate skin barrier disruption caused by the transdermal patches. *In vivo* studies evaluated the pharmacokinetic characteristics of SS in the transdermal patch formulation, as well as the pharmacokinetic characteristics of intravenous (i.v.) and oral administration in rats for comparison.

1.1. Materials

SS was purchased from Jiudian Pharmaceutical Co., Ltd. (Hunan, China). Nikasol TS620 was purchased from Nippon Carbide Industries Co., Inc. (Tokyo, Japan). HGA 64 was kindly provided by CosMED Pharmaceutical Co., Ltd. (Kyoto, Japan). Cosmetic concentrated glycerin was purchased from Miyoshi&Oil Fat Co., Ltd. (Tokyo, Japan). Pentobarbital sodium was purchased from Kyoritsu Seiyaku Corp. (Tokyo, Japan). Acetonitrile and ammonium dihydrogen phosphate were purchased from Wako Pure Chemical Industries, Ltd. (Osaka, Japan). DIAFOIL® polyester film (thickness 26 μm) was supplied by Mitsubishi Plastics, Inc. (Tokyo, Japan). Polyethylene terephthalate film (SPPET7501BU, thickness 75 μm) was purchased from Panac. Co., Ltd. (Tokyo, Japan). All other chemicals and reagents were of analytical reagent grade and commercially available.

Male Wistar rats (8 weeks old, 200 to 250 g) were purchased from Shimizu Laboratory Supplies Co., Ltd. (Kyoto, Japan). All experiments were performed in accordance with the guidelines of the Animal Ethics Committee at Kyoto Pharmaceutical University.

1.2. Fabrication of SS-incorporated patches

1.2.1. Methods

Two types of transdermal patches containing SS were fabricated, using either emulsion Nikasol TS620 (SS Nikasol patch) or hydrophilic acrylic adhesive HGA 64 (SS HGA patch), as shown in Fig. 2. In detail, SS was completely dissolved in distilled water. The adhesive and a solubility modifier (glycerin) were added to the drug solution and mixed well. In order to increase the solvent evaporation rate, suitable ethanol was added and mixed thoroughly to obtain a homogeneous coating formulation. Air bubbles were removed using a mix-rotor (MR-3, As One Corp., Osaka, Japan). After bubbles were completely removed, the formulation was coated onto the backing membrane (DIAFOIL® polyester film) using a knife coater (SKP 5702, Werner Mathis Ag, Oberhasli, Switzerland) and then dried in a convection

oven at 100 ℃ for 20 min (SS Nikasol patch) or 80 ℃ for 10 min (SS HGA patch) to remove residual water and organic solvents. The release liner (polyethylene terephthalate film) was laminated on the dried matrix. The morphology and crystallization of patches was observed using a stereoscopic microscopy (M205C, Leica Microsystems Ltd., Wetzlar, Germany).

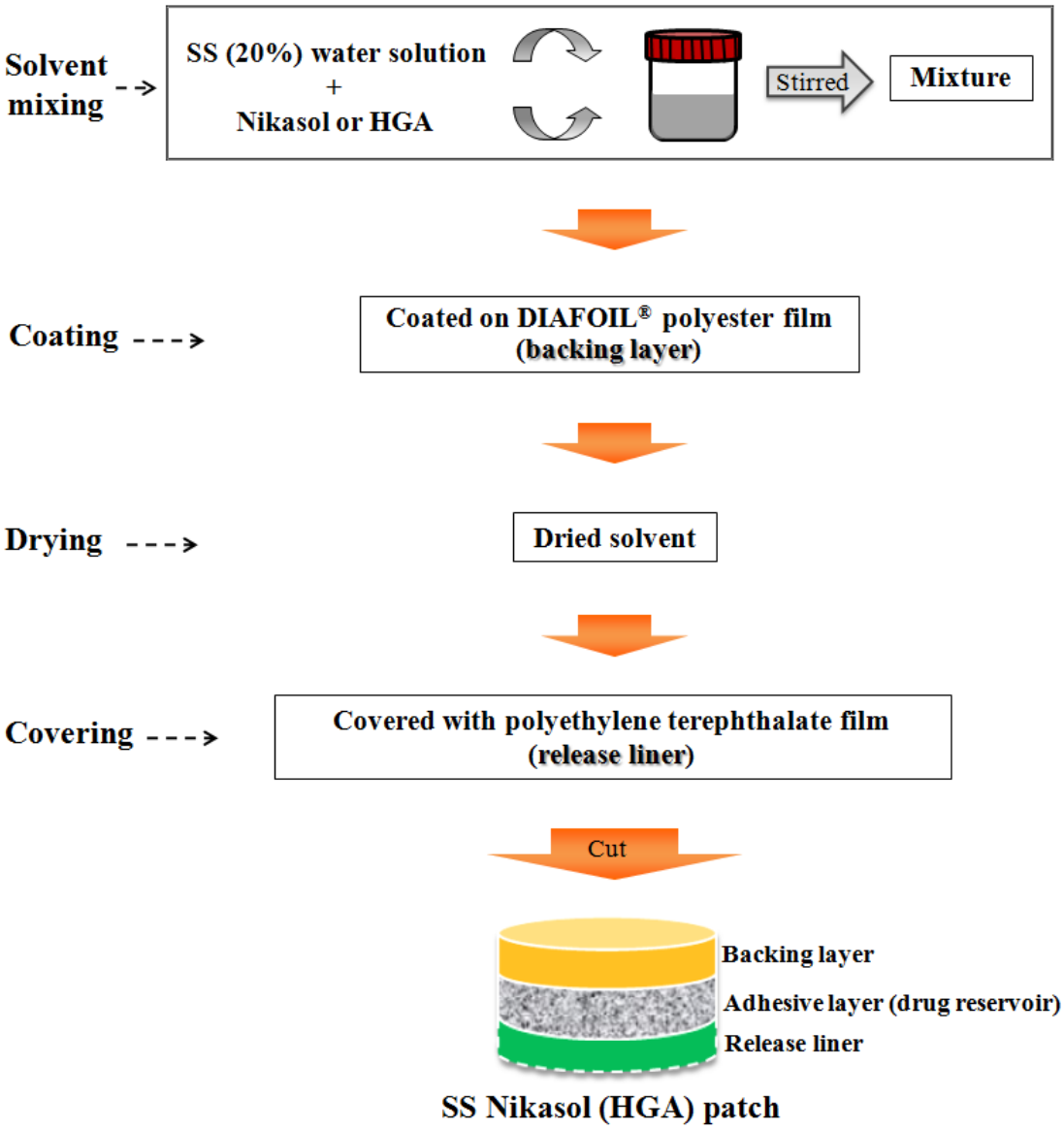

Fig. 2. Fabrication procedure of the SS-incorporated patches.

1.2.2. Results

As shown in Fig. 3A and Fig. 3B, SS possessed good compatibility with two types of

adhesives at content of 20% (w/w), and SS was dissolved in both adhesives with a uniform distribution. However, when SS was incorporated up to 25%, the formation of crystallization in the Nikasol adhesive layer was observed visually as well as by stereoscopic microscopy after 2 weeks (Fig. 3C). Therefore, based on the above reasons, as the SS content, 20% was chosen.

The dried thickness of the patches used ranged from 40 to 45 μm, which was determined using a thickness gauge (TH-102, Tester Sangyo Co., Ltd., Saitama, Japan) and was calculated by subtracting the combined thickness of the backing membrane and release liner from the whole patch thickness.

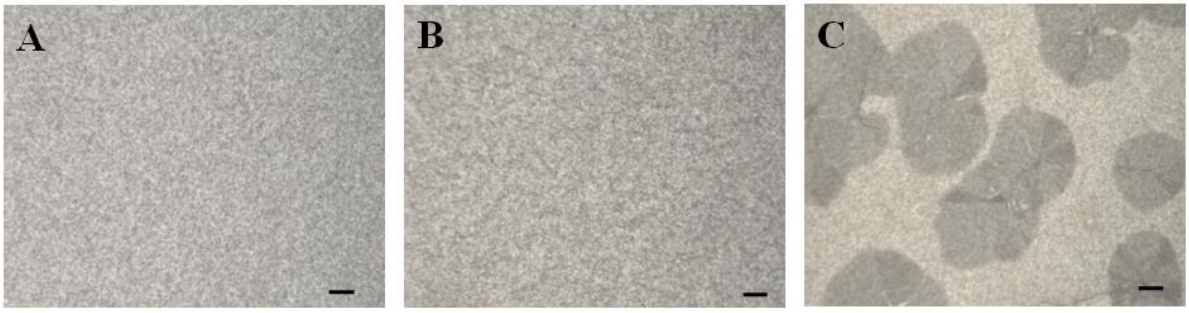

(Journal of Drug Delivery Science and Technology, Figure 2)

Fig. 3. Micrographs of sumatriptan succinate (SS)-incorporated patches after preparation. (A) SS Nikasol patch containing 20% SS, (B) SS HGA patch containing 20% SS, (C) SS Nikasol patch containing 25% SS after storage at room temperature for 2 weeks. Bars = 300 μm.

1.3. Determination of SS contents in SS-incorporated patches

1.3.1. Methods

Both types of patches were cut into circular shape (area 0.785 cm^2, diameter 10 mm). Each patch sample was weighed accurately and immersed in 10 mL of pH 7.4 phosphate buffered saline (PBS), and then sonicated and vortexed adequately. The release liner was separated from the adhesive layer before extraction. The drug content of each patch sample

was determined using a high performance liquid chromatography (HPLC) system (Shimadzu DGU-20A3, Kyoto, Japan) equipped with a UV detector (Shimadzu SPD-20A, Kyoto, Japan) and a reverse phase column (Cosmosil 5C18-PAQ, 4.6 mm × 150 mm, Nacalai U.S.A., Inc., San Diego, U.S.A.). The mobile phase consisted of acetonitrile and 0.5 M ammonium dihydrogen phosphate solution pH 3.3 (5:95). A flow rate of 1.0 mL/min was maintained, column temperature was 40 ℃, and the detection wavelength was 228 nm.

1.3.2. Results

The contents of SS in Nikasol patch and HGA patch were 99.8 ± 1.8% and 99.1 ± 2.3% (mean ± S.E., n = 6), respectively. Amount of SS in both types of patches was 1.53 mg/cm^2. SS was precisely loaded in both patches in accordance with each dosage with the standard error below 3%.

1.4. Measurement of adhesion properties of SS-incorporated patches

1.4.1. Methods

To determine the adhesion properties of the SS-incorporated patches, peel adhesion force and tackiness were measured according to the method described by Ah et al. [21] with slight modification. In brief, a texture analyzer (SV-52N-50, Imada Seisakusho Co., Ltd, Aichi, Japan) was used for the determination. Peel adhesion force was measured using the 180 ° peel adhesion test. Patches were cut (2.5 cm × 20 cm) and then applied to a plastic plate. The patches were smoothened with a 0.5 kg roller 3 times and allowed to adhere for 30 min prior to being pulled from the substrate at a 180 ° angle, at a rate of 120 mm/min. The tackiness of the patches was measured by the probe tack test. Patches were cut (3 cm × 3 cm) and attached to a stainless steel plate. After touching the adhesive layer with a cylindrical probe (diameter 10 mm), the probe was moved back at a rate of 20 mm/min, and the maximum strength was recorded.

1.4.2. Results

Peel adhesion forces of the SS Nikasol patch and the SS HGA patch were 756.7 ± 10.5 g/2.5cm and 676.7 ± 44.8 g/2.5cm (mean ± S.E., n = 6), respectively. During the test, both types of SS patch were stripped cleanly from the plate and left no noticeable residue. The tack values of the SS Nikasol patch and the SS HGA patch were 372.2 ± 13.2 g and 288.3 ± 54.7 g (mean ± S.E., n = 6), respectively. There were no significant difference in the peel adhesion force or tack values between the SS Nikasol patch and the SS HGA patch ($P > 0.05$). These results suggested that both SS-incorporated transdermal patches had good adhesive properties.

1.5. *In vitro* transdermal permeation of SS from SS-incorporated patches

1.5.1. Methods

In vitro skin permeation tests were performed using a vertical Franz diffusion cell with an effective diffusion area of 0.95 cm^2 (FTB-02, FINE Co. Ltd., Osaka, Japan). The abdominal hair of rats was shaved using a razor (Braun GmbH, Kronberg, Germany), following removal of hair by an electric clipper (model 900, TGC Inc., Daito, Japan). The full-thickness of the skin (i.e., epidermis with stratum corneum and dermis) was excised while the animals were anesthetized with pentobarbital sodium (35 mg/kg). Human abdominal skin was obtained from the International Institute for the Advancement of Medicine (Jessup, PA, U.S.A.). The following studies were conducted in agreement with the Ethical Committee of the Kyoto Pharmaceutical University and informed patient consent. The subcutaneous fat and other extraneous tissues of human or rat skin were trimmed and removed. A piece of excised skin (human or rat, area 3.14 cm^2, diameter 20 mm) was mounted on the Franz diffusion cell with the stratum corneum facing the donor compartment. One circular SS Nikasol or SS HGA patch (area 0.785 cm^2, diameter 10 mm) was applied to the stratum corneum side of the skin. The receptor compartment was filled with 3 mL of pH 7.4 PBS and maintained at 32 ℃ using a circulating water bath stirred with magnetic bars. At predetermined intervals, 0.3 mL of the

receptor solution was withdrawn and replaced with an equal volume of fresh medium. The concentration of SS was analyzed using an HPLC system as described above.

1.5.2. Results

The cumulative SS permeation profiles from the transdermal patches through rat skin are shown in Fig. 4A. The mean cumulative permeation of SS from the SS Nikasol patch and SS HGA patch after 24 h was found to be 745.9 ± 21.5 μg/cm^2 and 224.3 ± 68.4 μg/cm^2, respectively (Fig. 4A(a)).The cumulative permeation of SS from the SS Nikasol patch was significantly higher than that of the SS HGA patch ($P < 0.05$). Correspondingly, as shown in Fig. 4A(b), the SS Nikasol patch had a significantly higher maximum transdermal flux value (99.8 ± 29.8 μg/cm^2·h) than that observed with the HGA patch (10.8 ± 7.9 μg/cm^2 ħ) over a 24 h period ($P < 0.001$). Therefore, these results suggested that the permeability of SS from the Nikasol emulsion patch was greater than that of the HGA patch, making it an excellent candidate for the development of SS transdermal patches. Indeed, a similar trend in the *in vitro* release profiles of both patches were also obtained, where the Nikasol patch appeared a faster release rate compared with that of HGA patch in pH 7.4 PBS (data not shown).

The cumulative SS permeation profiles from the SS Nikasol patch through human skin are presented in Fig. 4B. The amount of SS that permeated through human skin was significantly lower than rat skin ($P < 0.001$), as the mean cumulative permeation was 9.8 ± 0.8 μg/cm^2 (Fig. 4B(a)) within 24 h. A significant increase/decrease in the maximum transdermal flux value (5.6 ± 0.5 μg/cm^2 ħ) was also seen in Fig. 4B(b) after application of the Nikasol patch to human skin, indicating that SS was quickly released from the Nikasol emulsion patch. Additionally, it was difficult to detect the permeated amount of SS from the HGA patch in the receptor compartment, because of the limit of detection of the HPLC system in our laboratory; hence, the permeation was assumed as zero.

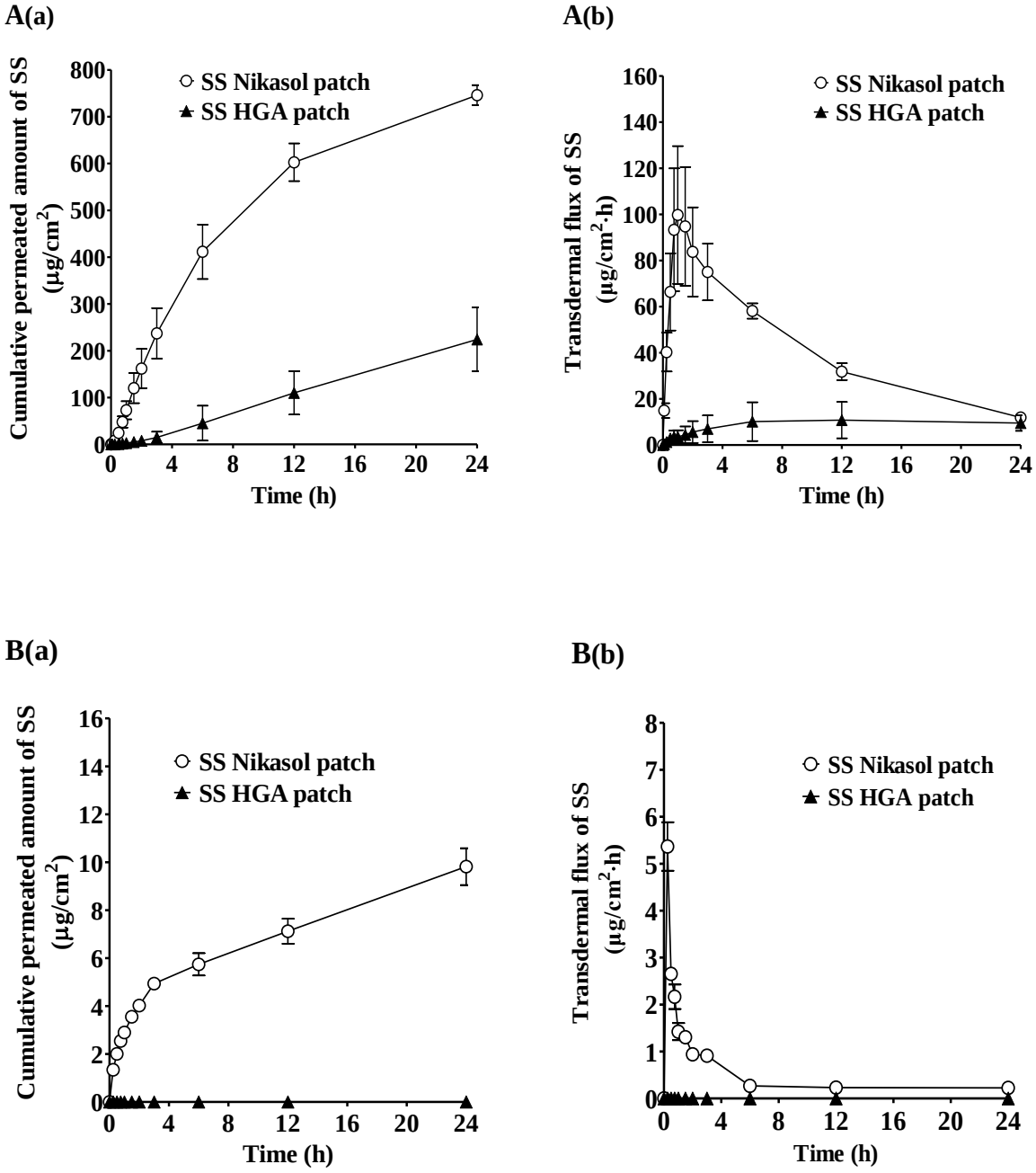

(Journal of Drug Delivery Science and Technology, Figure 3)

Fig. 4. *In vitro* cumulative permeated amount (a) and flux (b) of sumatriptan succinate (SS) through skin after application of the SS-incorporated transdermal patches in phosphate-buffered saline (pH 7.4) maintained at 32 ℃. (A) Permeation of SS from the Nikasol patch and HGA patch through rat skin, (B) Permeation of SS from the Nikasol patch through human skin. Results are presented as the mean ± S.E. of three to five rat or human tissue samples.

1.6. Assessment of rat skin barrier disruption after application of SS-incorporated patches via TEWL measurements

1.6.1. Methods

TEWL is an important index of skin disruption that occurs by various physical and chemical influences. Rats were acclimatized to the ambient temperature and relative humidity, which were 25 ± 2 ℃ and 50 ± 5%, respectively, for 30 min. Animals were anesthetized via an intraperitoneal injection of pentobarbital sodium (35 mg/kg) and abdominal hair was shaved using an electric clipper and a hair razor. Just before treatment, healthy rats without signs of scratches or illness were chosen. Circular SS patches with diameter of 20 mm were applied for a period of 24 h and were covered with absorbent gauze and fixed using adhesive bandage. The treatment sites on the shaved rats were marked as circular areas (~3.14 cm^2) with a marker. TEWL values were measured on rat skin via a Tewameter (TM 300, Courage and Khazaka Electronic GmbH, Cologne, Germany). A probe was applied to the skin. TEWL values represented the mean readings for 20 s before the measurements were automatically stopped. The values were determined before application and after removal of patches at the indicated time intervals over a period of 4 d. TEWL values were also determined over similar time intervals for the control group (i.e., without patch treatment).

1.6.2. Results

To determine whether skin barrier function was disrupted following application of two types of transdermal patches containing SS, TEWL values of the rat skin were measured before treatment and after removal of the patches, at the indicated times over a 4 d period (Fig. 5). The mean TEWL value of untreated skin was 4.28 ± 0.74 g/h·m^2. Rats were treated with patches for 24 h. Following the removal of the patches (0 h), the mean TEWL value of the Nikasol patch was increased to 8.86 ± 1.86 g/h·m^2 ($P > 0.05$), whereas as application of the HGA patch increased the mean TEWL value to 10.63 ± 0.64 g/h·m^2 ($P < 0.05$), compared

with the control group. However, the mean TEWL values gradually decreased back to baseline ($P > 0.05$) within 72 h after application of SS Nikasol patch or SS HGA patch. There was no significant difference ($P > 0.05$) between the values of the SS Nikasol patch group and the SS HGA patch group over the course of the experimental period. In addition, no visible irritation was appeared after application of both types of the SS-incorporated transdermal patches to the rat skin within the time frame of the experiment, as compared to the normal skin (Fig. 6).

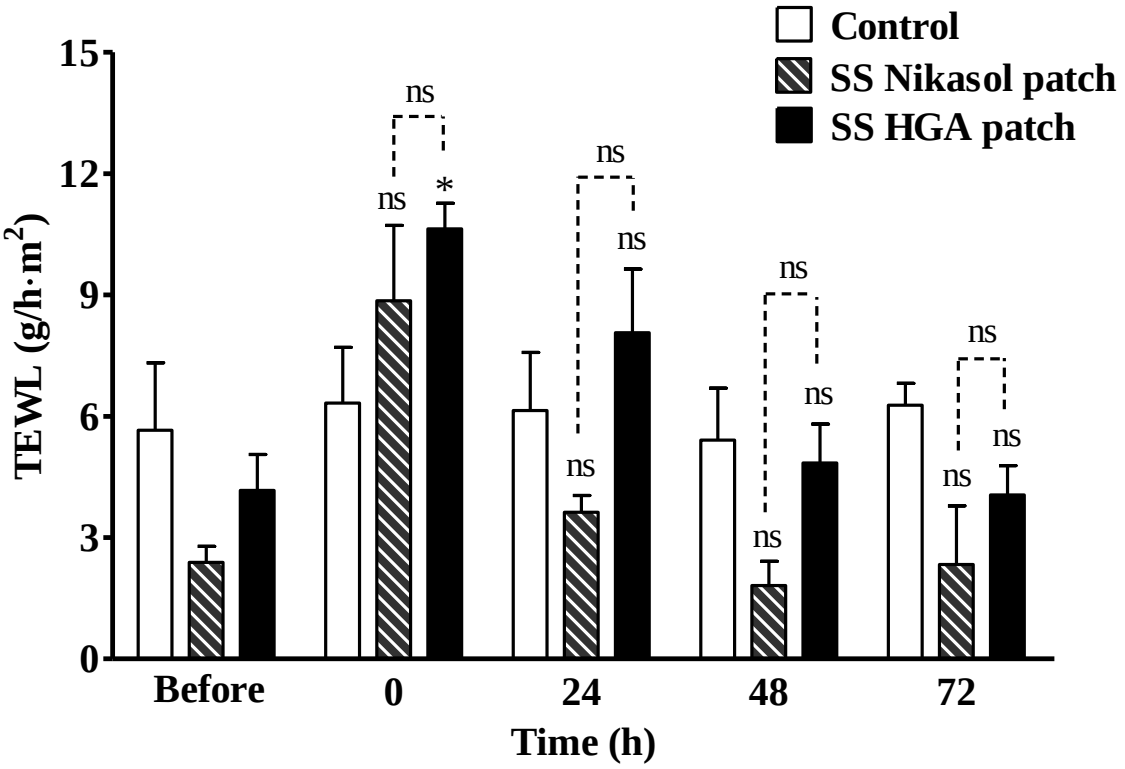

(Journal of Drug Delivery Science and Technology, Figure 4)

Fig. 5. Transepidermal water loss (TEWL) values of rat skin before application and 0-72 h after removal of sumatriptan succinate (SS) Nikasol patch and SS HGA patch. Results are presented as the mean ± S.E. of three experiments. $^{*}P < 0.05$, compared with the control group. (ns) not significantly different, compared with the control group, or as compared between SS Nikasol patch group and SS HGA patch group.

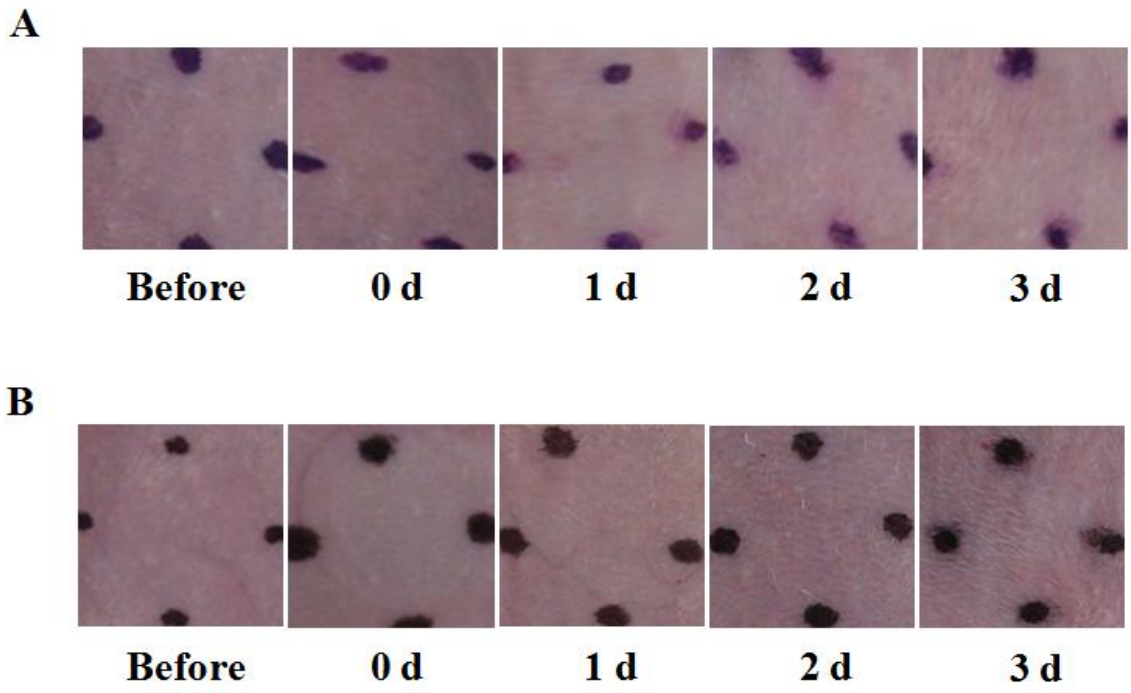

(Journal of Drug Delivery Science and Technology, Figure 5)

Fig. 6. Images of the rat skin before application and after removal of sumatriptan succinate (SS)-incorporated patches. (A) Typical examples of rat skin before application and 0-3 d after removal of SS Nikasol patch. Patch was applied for a period of 24 h, (B) Typical examples of rat skin before application and 0-3 d after removal of SS HGA patch. Patch was applied for a period of 24 h.

1.7. *In vivo* transdermal absorption of SS from SS-incorporated patches

1.7.1. Methods

Male Wistar rats were fasted for 12 h before treatment, while being provided water *ad libitum*. All animals were anesthetized via an intraperitoneal injection of pentobarbital sodium (35 mg/kg). Rats were divided into the following groups: (1) SS i.v. group, where SS was dissolved in pH 7.4 PBS and injected intravenously into the left jugular vein (10 mg/kg), (2) SS oral group, where SS was dissolved in pH 7.4 PBS and administrated using an intragastric needle (40 mg/kg), (3) SS Nikasol patch group, where two circular SS Nikasol patches with a total area of about 6.28 cm^2 (individual is 3.14 cm^2 with a diameter of 20 mm) containing 9.6

mg SS were applied to the shaved skin and fixed with tape (39.7 mg/kg), and (4) SS HGA patch group, where two circular SS HGA patches with total area of about 6.28 cm^2 (individual is 3.14 cm^2 with a diameter of 20 mm) containing 9.6 mg SS were applied to the shaved skin and fixed with tape (40.2 mg/kg). For transdermal medication, the abdominal hairs were shaved using an electric clipper and a razor. Patch attachment was sustained for 24 h. Blood samples (0.5 mL) were collected from the femoral vein with a heparinized syringe at 0, 1, 5, 15, 30, 60, 120, 180 min after administration in the i.v. group, and from the jugular vein at 0, 15, 30, 45, 60, 120, 180, 360, 1440 min after administration in the oral and patch groups. Blood samples were centrifuged at 12000 rpm for 5 min to separate plasma immediately.

The plasma samples were treated according to the following methods. Plasma samples (100 μL) were mixed with 1 mL acetonitrile to precipitate protein and vortexed for 1 min. After centrifugation at 12000 rpm for 5 min, the clear supernatant layer was collected and evaporated with a micro-vacuum concentrator centrifuge (PV-1200, Wakenyaku Co., Ltd., Kyoto, Japan) to remove residual organic solvents. The dried substrates were reconstituted with 150 μL of pH 7.4 PBS and vortexed before injection to the HPLC system.

Pharmacokinetic parameters, such as the maximal plasma drug concentration (C_{max}) and time to maximal plasma drug concentration (T_{max}), were determined from the individual plasma concentration-time profiles. The area under the time-concentration curves ($AUC_{0\rightarrow 24h}$) was calculated by the linear trapezoidal rule method from zero to the last time point. Absolute BA was calculated according to the following equation:

$$BA\ (\%) = (AUC_{patch} \times Dose_{i.v.}) / (AUC_{i.v.} \times Dose_{patch}) \times 100$$

Where AUC_{patch} indicates the area under the time-concentration curve after applying the SS-incorporated patches, and $AUC_{i.v.}$ indicates the area under the time-concentration curve after intravenous injection of SS.

All statistical analyses were performed using GraphPad Prism software (GraphPad Software Inc., San Diego, CA., U.S.A.). Results are presented as mean ± S.E. A Student's unpaired *t*-test was used for comparisons between data points. Multiple data sets within groups were analyzed with a one-way analysis of variance (ANOVA) followed by a Dunnet's *post hoc* test. For all comparisons, $P < 0.05$ was considered to be statistically significant.

1.7.2. Results

The mean plasma concentration-time profiles of SS after i.v., oral and transdermal administration are presented in Fig. 7. SS rapidly disappeared from blood circulation after i.v. injection via the left jugular vein. Plasma concentration decreased to 0.47 ± 0.06 μg/mL at 3 h. SS was rapidly absorbed from the gastrointestinal tract following oral administration, as the plasma C_{max} of 0.66 ± 0.13 μg/mL was achieved at a T_{max} of 35.00 ± 5.31 min. In contrast, the plasma concentration of SS increased gradually during the first 6 h after application of the SS patches. The T_{max} for transdermal delivery was significantly greater than that for oral administration ($P < 0.001$). The plasma concentration of SS following transdermal delivery also declined more slowly than the plasma concentration after oral administration.

The pharmacokinetic parameters of SS after administration by different methods were calculated and summarized in Table 1. Compared with oral administration, the $AUC_{0\rightarrow 24h}$ values were increased in the transdermal Nikasol patch (379.11 ± 47.79 μg·min/mL for the transdermal SS Nikasol patch *vs.* 292.63 ± 18.83 μg·min/mL for oral administration, $P > 0.05$). After dose normalization, the absolute BA of SS after transdermal Nikasol patch administration was 28.46 ± 1.93%, while the absolute BA after oral administration was 21.80 ± 2.66%. There were significant differences between the $AUC_{0\rightarrow 24h}$ ($P < 0.01$) and BA ($P < 0.001$) values after transdermal administration of SS Nikasol patch *vs.* the SS HGA patch (60.32 ± 12.46 μg·min/mL and 4.47 ± 0.66%). These findings suggested that SS was effectively absorbed from the Nikasol patch through the skin.

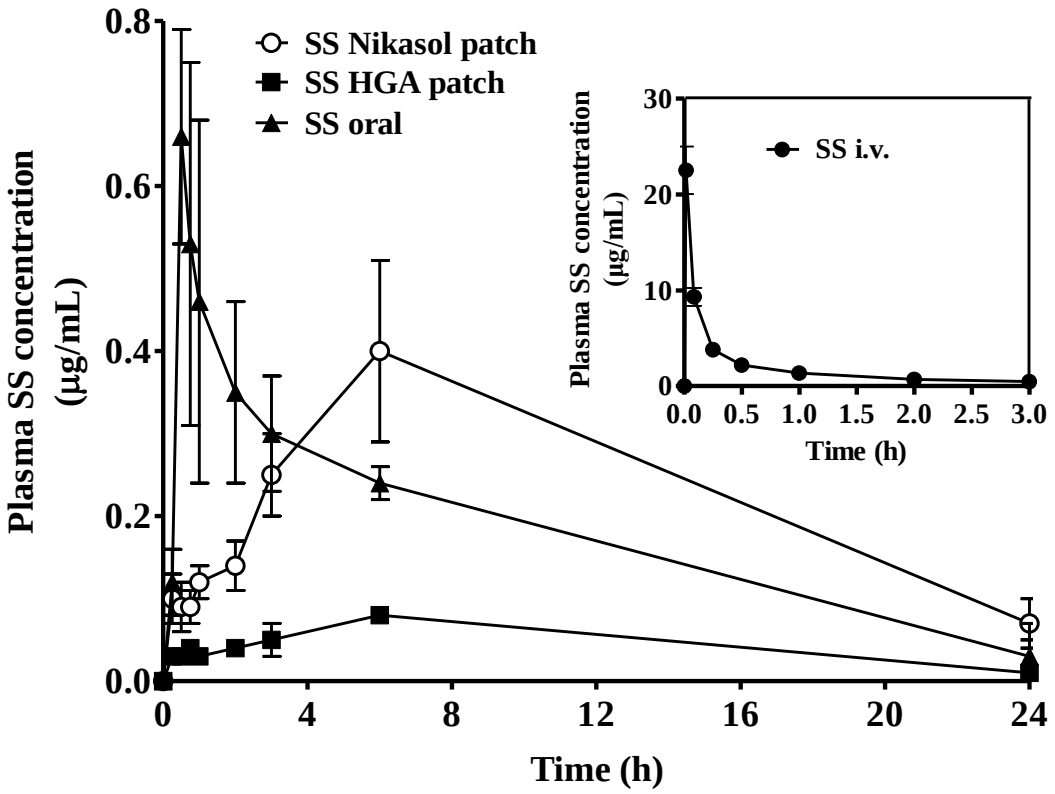

(Journal of Drug Delivery Science and Technology, Figure 6)

Fig. 7. Plasma concentration-time profiles after intravenous (i.v.), oral and transdermal delivery of sumatriptan succinate (SS) over a period of 24 h. Results are presented as the mean ± S.E. of three to four experiments.

Table 1. Pharmacokinetic parameters of sumatriptan succinate (SS) after intravenous (i.v.), oral, and transdermal administration.

Groups	C_{max} (μg/mL)	T_{max} (min)	$AUC_{0\rightarrow 24h}$ (μg·min/mL)	BA (%)
SS i.v.	-	-	335.53 ± 7.79	-
SS oral	0.66 ± 0.13	35.00 ± 5.31	292.63 ± 18.83	21.80 ± 2.66
SS Nikasol patch	0.40 ± 0.11	324.00 ± 22.20***	379.11 ± 47.79$^{\#\#}$	28.46 ± 1.93$^{\#\#\#}$
SS HGA patch	0.08 ± 0.01	300.00 ± 29.93	60.32 ± 12.46	4.47 ± 0.66

Results are presented as the mean ± S.E. of three to four experiments. *** $P < 0.001$ compared with oral group. $^{\#\#\#}$ $P < 0.001$ or $^{\#\#}$ $P < 0.01$ compared with SS HGA patch group. (Journal of Drug Delivery Science and Technology, Table I)

1.8. Discussion

The present study provided the first evidence for the use of Nikasol, an acrylic fiber system water emulsion resin, in the preparation of SS-incorporated patch, and showed that the patch could effectively improve the transdermal delivery of SS through skin.

A steady and continuous permeation of SS from all the patches was observed, indicating that SS was dissolved in all adhesives with a uniform distribution. It was found that the permeation of SS from the Nikasol patch was approximately threefold higher than that of the HGA patch through rat skin. One potential explanation for this effect was that, in the Nikasol patch, SS molecules were dispersed in the hydrophilic portion of the emulsion, instead of entering inside the hydrophobic polymer. After evaporation of moisture, drug molecules adsorbed on the surface of the lipophilic polymer, which easily passed through the skin barrier layer. Meanwhile, glycerin as the solubility modifier could lubricate the movement of the drug molecule, resulting in higher skin permeability. In contrast, SS molecules dissolved within the hydrophilic polymer of the HGA patch, resulting in difficulties in passing through the skin barrier. In addition, may be due to the different delivery mechanism of SS from both types of patches, a rapid increase in the flux values was obtained after application of Nikasol patch to rat or human skin, in contrast to the slow increase after application of HGA patch, indicating that SS was quickly released from the Nikasol system. These findings supported the idea that the selection of an emulsion adhesive played a decisive role in the percutaneous absorption of SS from the transdermal patches.

It was also noted that the permeation of SS through human skin was seventy-fold lower than permeation through rat skin, likely due to differences in the thickness and lipid component of the stratum corneum between rodents and humans [52,53]. It was known that the cumulative amount of SS that permeated through the human skin was 9.8 ± 0.8 $\mu g/cm^2$ after a 24 h application of the Nikasol patch. If the area of the patch for clinical use is calculated on the basis of the cumulative amount of SS permeated through the human skin

during a 24 h application, a patch of 290 cm^2 would be able to deliver approximately 2.9 mg of SS, which is approximately equivalent to the amount of SS absorbed by single dose 20-mg intranasal administration in clinical use [54]. According to a report by Mazières et al. [55], ketoprofen patches with an area of 50 to 400 cm^2 are usually applied to the patients for clinical use. However, patches with an area near 300 cm^2 are often inconvenient, and may reduce patient compliance. Therefore, further studies with the preparation of SS-loaded MNs were conducted as an alternative method to improve the transdermal absorption of SS. Nevertheless, though the percutaneous permeability needs to be further improved, our results suggest that the transdermal permeation of SS using our Nikasol emulsion patch system may be promising for the treatment of migraine.

TEWL is an important index for the investigation of skin disruption after the application of transdermal patch systems [56,57]. In the present study, we found that TEWL immediately increased after the removal of transdermal patches. However, the increase in TEWL gradually recovered to baseline levels after 72 h during the experimental period. These findings corroborate the previous report of Fokuhl and Müller-Goymann [58]. It is generally known that an increase in TEWL results from a reduction in the skin barrier, leading to an evaporation of water from the skin, potentially causing intracellular gaps in the stratum corneum to temporarily loosen. Combined, these results indicate an increase in skin permeability, and support the successful permeation of SS from the patches through rat skin. According to a report by Kanikkannan et al. [59], both TEWL and percutaneous absorption rates increase when the integrity of the stratum corneum barrier is compromised. Furthermore, the Nikasol patch showed a less increase in TEWL values than the HGA patch, suggesting lower skin barrier damage. Additionally, the pictures of the skin surface also indicated no visible changes to the rat skin following treatment with SS-incorporated patches.

The pharmacokinetic characteristics of the SS transdermal Nikasol patches exhibited many advantages over other formulations. The low T_{max} and high C_{max} values following oral

administration were due to rapid absorption or significant first-pass metabolism by the gastrointestinal tract. The pharmacokinetic profiles indicated that the whole blood concentration of SS declined rapidly and, as a result, produced a short duration of therapeutic action. In contrast, the prolonged T_{max} and low C_{max} values following transdermal delivery may be owing to the continuous replenishment of SS in the systemic circulation by controlled delivery of the drug from the transdermal patch. This may be a benefit of the transdermal patch, because it requires less frequent dosing. Further, compared with other routes, the slow decline in blood concentration of SS after transdermal administration could be attributed to the reservoir effect of skin, resulting in slow depletion of the drug accumulated in skin tissues [60,61]. The SS Nikasol patch was also more advantageous than oral administration because the absolute BA value was approximately 1.3 times greater, which suggested the novel patch system effectively improved the transdermal absorption of SS. Previous studies suggest that higher BA may correspond to improved clinical benefits. For example, these parameters are associated with fewer adverse effects and consistent migraine pain relief [4,62]. We observed that there was significant difference of pharmacokinetic characteristics between the Nikasol patch and the HGA patch, which was consistent with the *in vitro* skin permeation results. These may be due to the different delivery mechanism of SS from both types of patches across the skin as mentioned above, and the *in vitro* faster release rate as well as higher *in vivo* absorption rate of SS from Nikasol patch than that of HGA patch. These findings suggest that the novel transdermal patch is an excellent candidate for delivering SS to migraine patients. However, it is generally known that there are great species differences between humans and rodents, further pharmacodynamic studies are needed to confirm whether the transdermal patch system is able to prevent migraine clinically.

It was demonstrated that the patch using Nikasol, an acrylic fiber system water emulsion resin, as an adhesive could be utilized to enhance transdermal delivery of SS. Compared with oral administration, the transdermal patch for SS delivery is an improved alternative to avoid

the difficulty in oral intake of SS because of nausea and vomiting that accompany with migraine, and to avoid pre-systemic metabolism, achieving a consistent plasma concentration over an extended period of time.

CHAPTER 2 Development of a novel self-dissolving MN loaded with SS

As mentioned earlier, it is difficult to delivery therapeutic amounts of SS from reasonably sized patches by passive diffusion across the skin. Hence, a novel self-dissolving MN fabricated from sodium hyaluronate with SS containing in whole needles was developed as a new alternative transdermal system. The MNs improved transport of SS by creating micro-scale pathways after insertion into the skin, combing the advantage of transdermal patches and hypodermic needles. Given that skin possesses intrinsic elastic proprieties, microneedles with specific geometry are necessary to penetrate the skin without any bending or breaking. To improve the mechanical strength, needles of tapered-cone shape with sharp tips were designed. Moreover, appropriate mechanical force must be applied to ensure homogeneous insertion the skin in the MN application. In this study, MNs were applied into the skin by an applicator. The applicator can apply MNs into the skin with a definite force (15 N/cm^2), and the force is enough for the insertion of MNs into the skin. With this applicator, the energy applied on MNs is well controlled, and is convenient to be self-administration.

In the present study, in order to improve permeability of SS from the SS-loaded MNs, *in vitro* permeation studies were conducted with excised human cadaver skin using vertical Franz diffusion cells and various parameters such as needle length, thickness, and density as well as penetration enhancers were investigated. The effect of SS-loaded MN hygroscopy on their mechanical strength was measured. Moreover, skin penetration characteristics and subsequent dissolution of the MNs after application onto rat skin were evaluated using optical coherence tomography (OCT). To assess the disruption and recovery of skin barrier function after administration of MNs, TEWL was measured. The resealing of micropores created by insertion of MNs *in vivo* was also observed. Furthermore, transdermal absorption characterizations of SS from MNs were evaluated and compared with that observed after s.c. injection or oral administration.

2.1. Materials

SS was purchased from Viwit Pharmaceutical Co., Ltd. (Shanghai, China). Sodium hyaluronate (Japanese Pharmacopoeia [JP] grade) was purchased from Kikkoman Biochemifa Company (Tokyo, Japan). L-(+)-Tartaric acid was purchased from Kanto Chemical Co., Inc. (Tokyo, Japan). Cosmetic concentrated glycerin was purchased from Miyoshi & Oil Fat Co., Ltd. (Tokyo, Japan). Sodium lauryl sulfate was purchased from Nacalai Tesque, Inc. (Kyoto, Japan). Lauric acid diethanolamide was purchased from Kao Corporation (Tokyo, Japan). Acetonitrile and ammonium dihydrogen phosphate were purchased from Wako Pure Chemical Industries, Ltd. (Osaka, Japan). All other chemicals and reagents were of analytical reagent grade and commercially available.

Male Wistar rats (8 weeks old, 250-270 g) were purchased from Shimizu Laboratory Supplies Co., Ltd. (Kyoto, Japan). All experiments were performed in accordance with the guidelines of the Animal Ethics Committee at Kyoto Pharmaceutical University.

2.2. Fabrication of sodium hyaluronate MNs

2.2.1. Methods

The MNs without any model component (placebo), and containing SS or blue dye, were fabricated by micromolding technologies with sodium hyaluronate as a base material, as shown in Fig. 8. In detail, sodium hyaluronate solution was obtained by thorough mixing with distilled water. Either SS (with or without penetration enhancers) or blue dye solution, dissolved in 3% tartaric acid, was added to the sodium hyaluronate solution and uniformly mixed. A small aliquot of the resulting solution was carefully cast in micromolds and dried in a desiccator at room temperature. After drying the micromolds completely, a polyethylene terephthalate adhesive tape was attached to the base plate for reinforcement. The SS- or blue dye-loaded MNs were obtained by peeling the mold off and cutting to a circular area with a diameter of 10 mm using a punch. MNs with different length, thickness or density were also

fabricated in the same manner using variety micromolds.

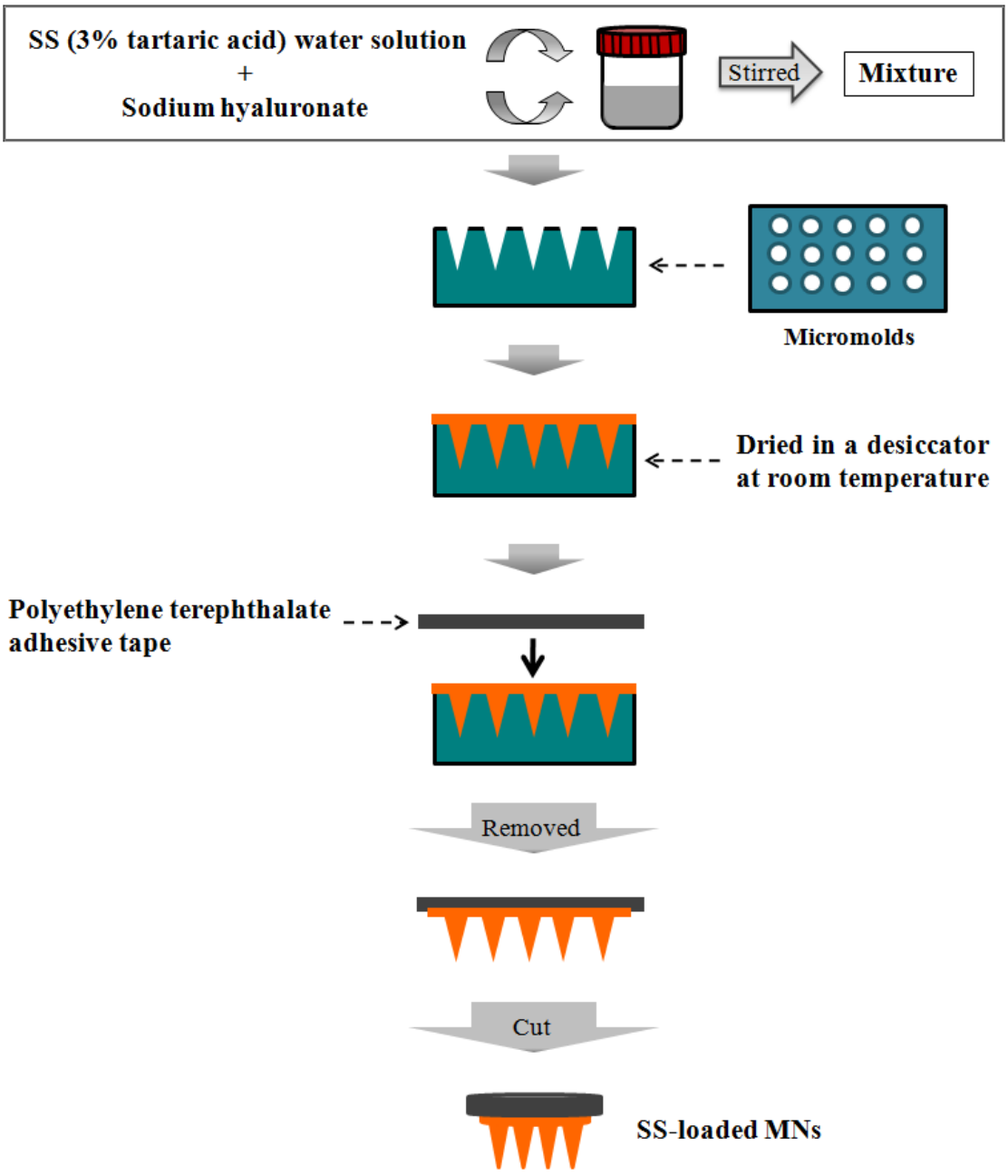

Fig. 8. Fabrication procedure of sumatriptan succinate (SS)-loaded microneedle arrays (MNs).

2.2.2. Results

Five types of MNs with different needle length, thickness, density and penetration enhancers were prepared. All the needles were tapered cone-shaped in a circular array with a diameter of 10 mm. Firstly, MNs with the length of 500 μm were designed to have

approximately 200 needles per array, basal diameter was 100 μm, tip diameter was 35 μm, and interspacing between needles was 600 μm. Secondly, as shown in Fig. 9, the named "800 usual MNs" with the length of 800 μm were designed to have about 200 needles per array, basal diameter was 150 μm, tip diameter was 35 μm, and interspacing was 600 μm. Thirdly, penetration enhancers-contained MNs were prepared with the same micromolds as the 800 usual MNs. Fourthly, the named "800 thick MNs" were designed to have around 200 needles per array, basal diameter was 170 μm, tip diameter was 45 μm, and interspacing was 600 μm. Lastly, the named "800 high density MNs" were designed to have approximately 500 needles per array, basal diameter was 110 μm, tip diameter was 25 μm, and interspacing between needles was 350 μm.

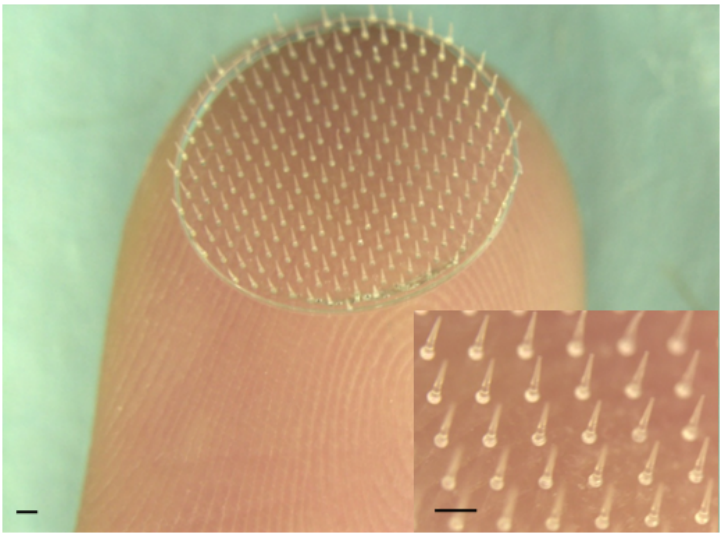

Fig. 9. Micrograph of an 800 μm usual microneedle array (MN) with a diameter of 10 mm. Bars = 500 μm.

2.3. Improvement of transdermal delivery of SS from SS-loaded MNs

2.3.1. Methods

In vitro skin permeation studies were performed using vertical Franz diffusion cells with a diffusion area of 3.14 cm^2. Human cadaver skin was obtained from the Biological Resource

Center, Inc. (Phoenix, U.S.A.). The subsequent studies were conducted in agreement with the Declaration of Helsinki, with informed patient consent, and were approved by the Ethical Committee of the Kyoto Pharmaceutical University. Residual subcutaneous fat and other extraneous tissues of human skin were trimmed to a thickness of 1000 μm using a surgical electric dermatome (B. BRAUN Melsungen AG, Melsungen, Germany). A piece of circular excised human skin (diameter 25 mm) was placed onto an equally sized piece of filter paper (stratum corneum uppermost). SS-loaded MNs were applied to the center of the skin. These skin membranes with the MNs in place were mounted on the Franz diffusion cells with the stratum corneum facing the donor compartments. The receptor compartments were filled with 2.4 mL of pH 7.4 PBS and maintained at 32 ℃ under stirring with magnetic bars. At predetermined intervals, 0.5 mL of the receptor solution was withdrawn and replaced with an equal volume of fresh medium. Sink conditions were maintained throughout all experiments.

The concentration of SS was analyzed on a HPLC system (Hitachi L-7000, Kyoto, Japan) equipped with a UV detector (Hitachi L-7405, Kyoto, Japan). A reverse phase C18 column (4.6 mm × 250 mm, Shiseido Co., Ltd., Tokyo, Japan) was used. The mobile phase was consisted of acetonitrile and 0.5 M ammonium dihydrogen phosphate solution pH 3.3 (5:95). A flow rate of 1.0 mL/min was maintained, column temperature was 40 ℃, and the detection wavelength was 228 nm.

2.3.2. Results

2.3.2.1. Effect of needle length on the skin permeation of SS

The effect of needle length on the transdermal delivery of SS was shown in Fig. 10. It was found that length of needles had a distinct effect on the permeation of SS. 800 μm MNs containing 9.8 mg SS/cm^2 showed an approximately three-fold increase in permeation of SS into the skin, compared with the case of 500 μm MNs containing 6.3 mg SS/cm^2 (Fig. 10A). Furthermore, as shown in Fig. 10B, SS was rapidly released from the MNs, when the length

of needles was increased from 500 to 800 μm, the maximum transdermal flux values significantly ($p < 0.05$) enhanced from 147.4 ± 2.7 to 386.8 ± 26.3 μg/cm^2 ħ at 1 h. These results suggested that the transdermal delivery of SS could be effectively improved by increasing the length of needles. Therefore, MNs with the height of 800 μm were employed for the following studies.

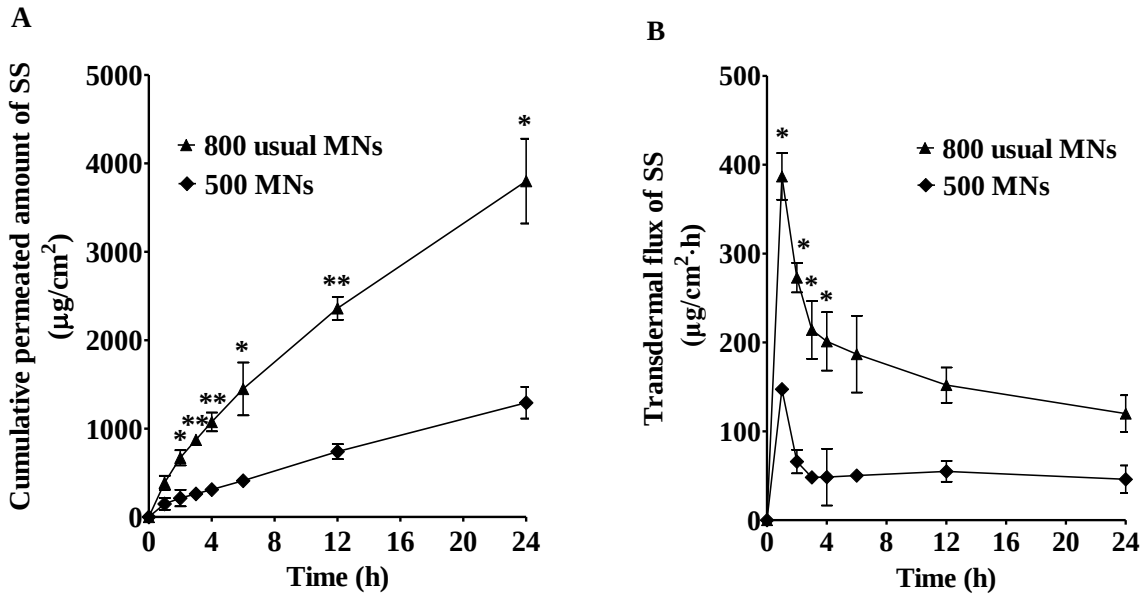

Fig. 10. *In vitro* cumulative permeated amount (A) and flux (B) of sumatriptan succinate (SS) delivered through human skin after application of SS-loaded microneedle arrays (MNs) with needle length of 500 μm and 800 μm, respectively. Results are presented as the mean ± S.E. of at least three experiments. $^{**}p < 0.01$, $^{*}p < 0.05$, compared with 500 MNs.

2.3.2.2. Effect of needle thickness on the skin permeation of SS

Further experiments were carried out to improve the transdermal delivery of SS from the SS-loaded 800 μm MNs. As shown in Fig. 11A, the mean cumulative permeation amount of SS from 800 usual MNs (9.8 mg SS/cm^2) and 800 thick MNs (11.2 mg SS/cm^2) at 4 h were found to be 992.0 ± 34.8 μg/cm^2 and 975.4 ± 47.2 μg/cm^2, respectively. There was no significant difference ($p > 0.05$) in cumulative permeation amount of SS over the 24 h period between the two types of MNs. Fig. 11B showed that SS was quickly released from the MNs,

and a maximum skin transdermal flux value was achieved at 1 h. These findings indicated that skin permeation of SS was not distinctly improved by increasing the thickness of MNs.

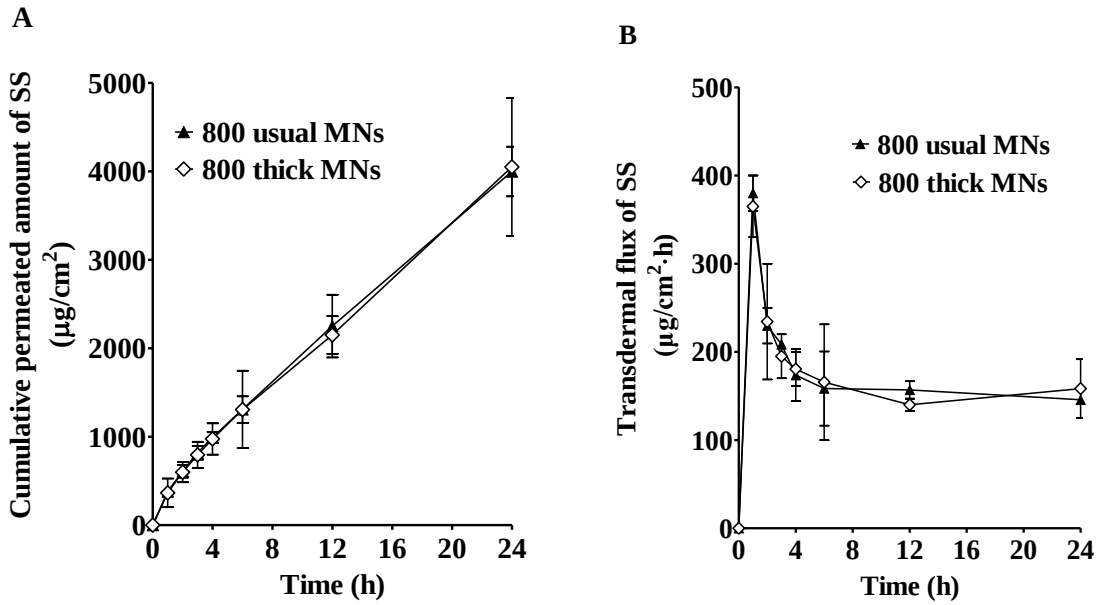

Fig. 11. *In vitro* cumulative permeated amount (A) and flux (B) of sumatriptan succinate (SS) delivered through human skin after application of SS-loaded 800 μm usual microneedle arrays (MNs) and 800 μm thick MNs. Results are presented as the mean ± S.E. of at least three experiments.

2.3.2.3. Effect of penetration enhancers on the skin permeation of SS

To improve the transdermal delivery of SS from the MNs, I tried to add 3% penetration enhancers in drug solution during preparation. Three kinds of enhancers were used including glycerin, sodium dodecyl sulfate (SDS) and lauric acid diethanolamide (LD), containing similar 9.8 mg SS/cm^2. As indicated in Fig. 12, SDS was appeared to be a relatively excellent enhancer compared with others. However, there was no significant difference ($p > 0.05$) in permeation of SS over the experimental period among all the MNs. These results suggested that the transdermal delivery of SS could not be effectively enhanced by the addition of penetration enhancers.

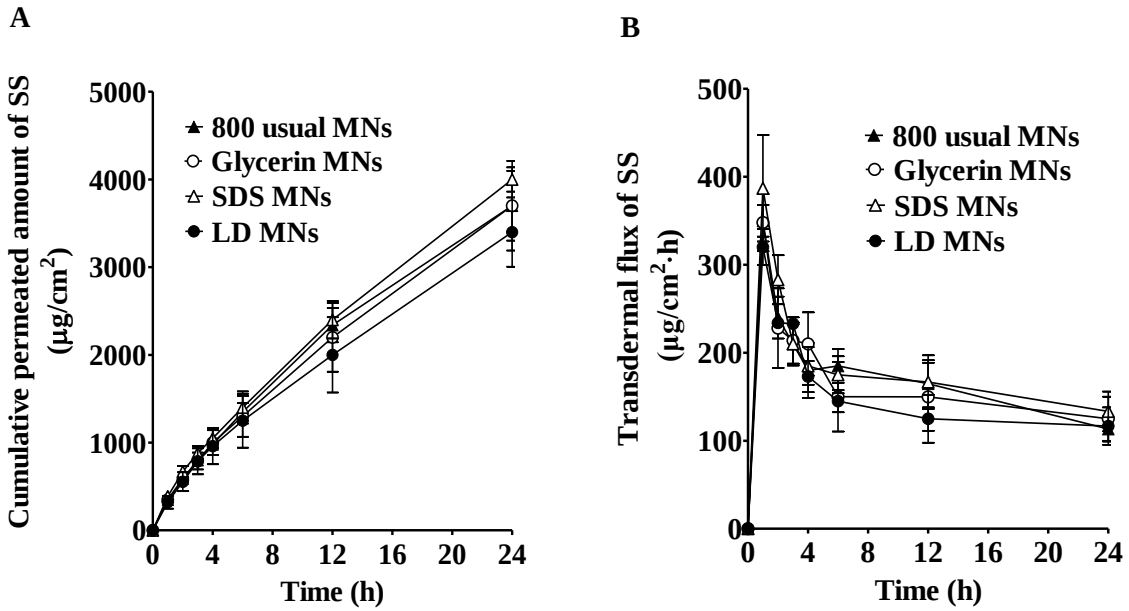

Fig. 12. *In vitro* cumulative permeated amount (A) and flux (B) of sumatriptan succinate (SS) delivered through human skin after application of SS-loaded 800 μm usual microneedle arrays (MNs), and the MNs containing 3% glycerin, sodium dodecyl sulfate (SDS) or lauric acid diethanolamide (LD) as penetration enhancers. Results are presented as the mean ± S.E. of at least three experiments.

2.3.2.4. Effect of needle density on the skin permeation of SS

Fig. 13A showed the *in vitro* cumulative permeated amount of SS after application of the high density MNs loading 11.0 mg SS/cm^2 and the usual MNs containing 9.8 mg SS/cm^2. The permeated amount of the high density SS-loaded MNs was up to 2150.6 ± 197.0 μg/cm^2 at 4 h, which was significantly higher ($p < 0.05$) than that obtained with the usual MNs (1040.4 ± 70.7 μg/cm^2). SS was speedily released from all the arrays (Fig. 13B). Therefore, combined the results of above *in vitro* skin permeated experiments together, we observed that the high density MNs with the needle length of 800 μm were able to provide our pre-needed permeated amount of SS into the skin.

For ease of description, the high MNs containing SS with needle length of 800 μm was

called for short as “SS-loaded MNs”, and were used for the subsequent studies.

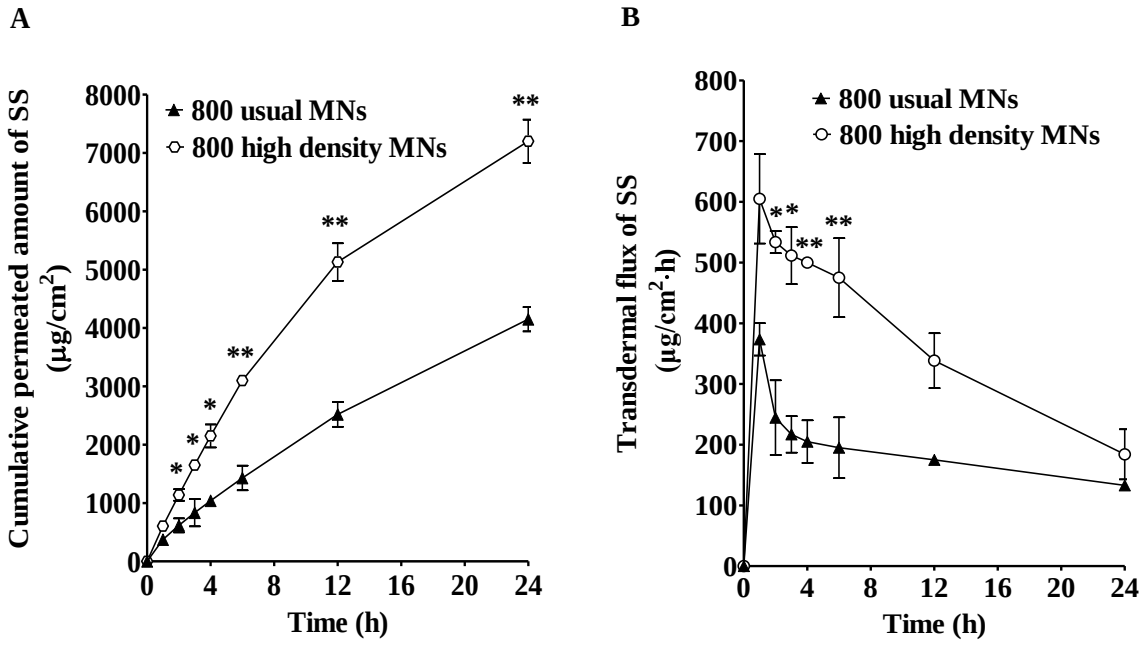

Fig. 13. *In vitro* cumulative permeated amount (A) and flux (B) of sumatriptan succinate (SS) delivered through human skin after application of SS-loaded 800 μm usual microneedle arrays (MNs) and 800 μm high density MNs. Results are presented as the mean ± S.E. of at least three experiments. $^{**}p < 0.01$, $^{*}p < 0.05$, compared with 800 usual MNs.

2.4. Measurement of mechanical failure force and hygroscopy of SS-loaded MNs

2.4.1. Methods

The mechanical failure force of SS-loaded MNs was measured using a texture analyzer (SV-52N-50, Imada Seisakusho Co., Ltd, Aichi, Japan). A single MN was attached to a lower test station, and the upper cylindrical movable probe then pressed the MN at a speed of 1.0-1.5 mm/min. The maximum force applied before immediate force drop was measured as the force of needle failure. Before and after the failure force test, all microneedles were examined by stereoscopic microscopy (M205 C, Leica Microsystems Ltd., Wetzlar, Germany).

To determine the hygroscopy of SS-loaded MNs, the arrays were stored in a desiccator containing a saturated solution of sodium chloride to achieve a relative humidity of 75%. MNs were removed at predetermined intervals, and their water content was measured using a moisture analyzer (MS-70, A&D Company, Limited (Japan), Tokyo, Japan). In addition, the mechanical failure force of the moisture-conditioned MNs was also determined.

2.4.2. Results

Fig. 14 shows the representative failure behavior of SS-loaded MNs under an axial load. Upon needle failure, the force declined suddenly, and the point before the sudden decrease was interpreted as the needle failure force, which was approximately 21 N. As shown in Fig. 15, after the failure force test, all needles were deformed with almost the same tip bending of 45 °, along with a displacement of approximately 200 μm. It was also observed that the microneedles was bending, whereas was not fracture, suggesting that the needles had sufficient toughness.

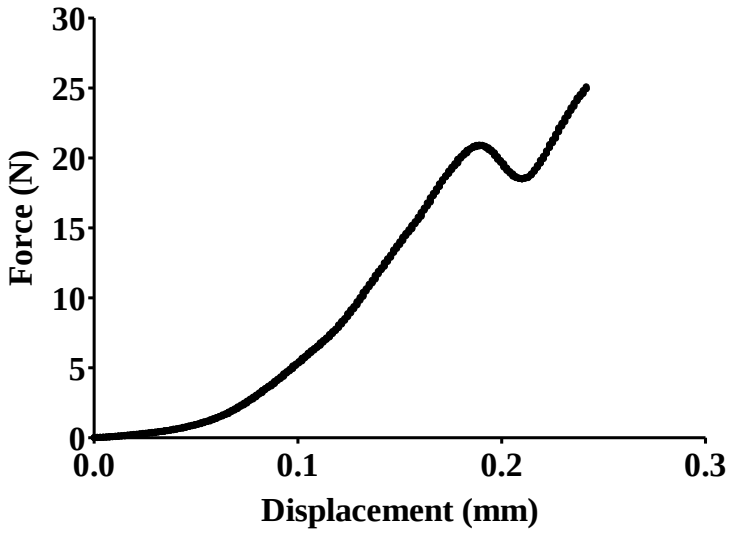

(Biological and Pharmaceutical Bulletin, Fig. 1)

Fig. 14. Force-displacement curve of sumatriptan succinate-loaded microneedle arrays under an axial load.

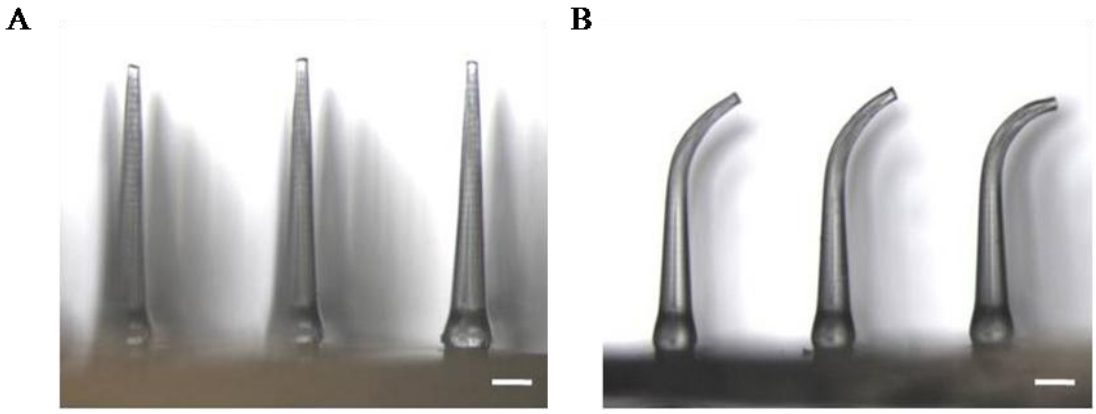

(Biological and Pharmaceutical Bulletin, Fig. 1)

Fig. 15. Bright micrographs of sumatriptan succinate-loaded microneedle arrays before (A) and after (B) an axial failure test. Bars = 100 μm.

Given that moisture had a great effect on the morphology and mechanical strength of soluble MNs, the hygroscopy of the SS-loaded MNs at a high relative humidity of 75% was measured. As shown in Fig. 16A, the mean water content of MNs before storage was 4.5%, and this value rapidly increased to 10.0% at 4 h. It was appeared that the absorption of moisture became saturated after 4 h. Correspondingly, the mechanical strength of the MNs declined as their water content increased (Fig. 16B). The mechanical strength declined quickly during the first 4 h, and then slowed down from 4 h to 24 h. When the water content increased to 10.0%, the failure force decreased to approximately 11.7 N per array. The increase in MNs water content due to absorption of moisture from the wet environment resulted in a softening of sodium hyaluronate materials, thereby decreasing their mechanical strength. Therefore, our MNs were stored in sealed aluminum laminated packages to prevent absorption of moisture. Further experiments showed that our MNs possessed sufficient strength to successfully penetrate the skin if the failure force was ≥ 16 N per array (data not shown), indicating that MNs maintained their insertion ability for at least 30 min, even at a relative humidity of 75%. Additionally, the structure of MNs did not change over the experimental period at the relative humidity of 75%.

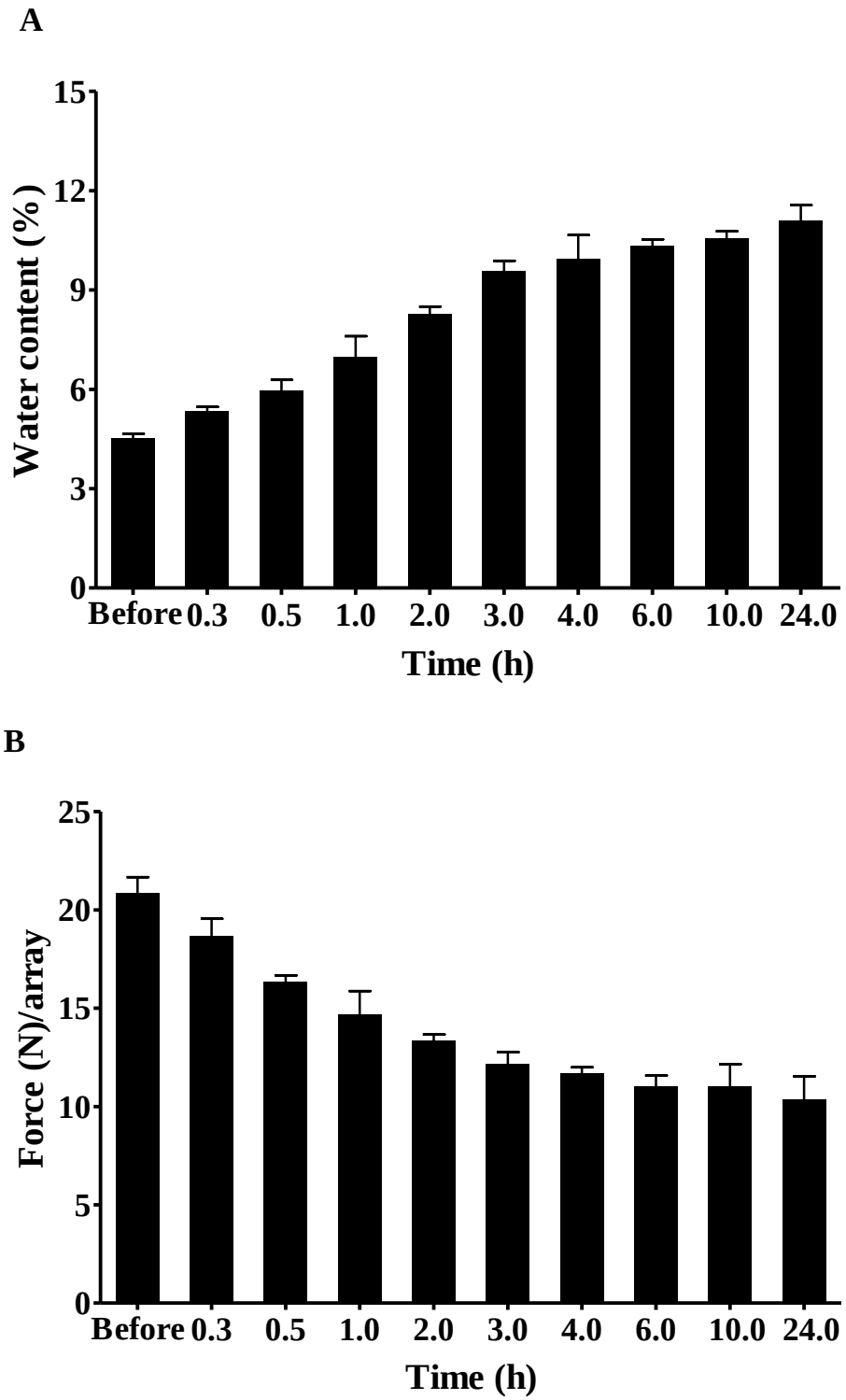

(Biological and Pharmaceutical Bulletin, Fig. 1)

Fig. 16. Water contents of sumatriptan succinate-loaded microneedle arrays after storage at a relative humidity of 75% over a period of 24 h (A). Mechanical failure force of the moisture-conditioned MNs (B). Results are presented as the mean ± S.E. of at least three experiments.

2.5. Estimation of skin penetration capacity of SS-loaded MNs

2.5.1. Methods

The penetration characteristics of high density SS-loaded MNs with the length of 800 μm following insertion into excised human skin were evaluated using OCT. Human cadaver skin was obtained from the International Institute for the Advancement of Medicine (Jessup, PA, U.S.A.). The following studies were conducted in agreement with the Ethical Committee of the Kyoto Pharmaceutical University and informed patient consent. Residual subcutaneous fat and other extraneous tissues of the skin were trimmed to a thickness of 1000 μm using a surgical electric dermatome (B. BRAUN Melsungen AG, Melsungen, Germany). SS-loaded MNs were inserted into the excised skin and left in place for 5 min. Upon removal of the arrays, the treated sites were immediately scanned using a Ganymede model OCT microscope (Thorlabs GmbH, Munich, Germany) to observe the puncturing capacity of the MNs.

2.5.2. Results

Fig. 17A shows a three-dimensional (3 D) image (volumetric scan) of the human skin surface after insertion of SS-loaded MNs. Orderly micropores were created *en face* with a pattern similar to the MNs. Fig. 17B shows a cross-sectional two-dimensional (2 D) image of the untreated human skin, which was intact prior to MNs application. As shown in Fig. 17C and Fig. 17D, distinct drug permeation pathways were created directly after the application of SS-loaded MNs to the skin. Moreover, skin pierced with MNs showed penetration depths of approximately 250-300 μm, which corresponded to insertion through the stratum corneum and epidermis and into the superficial dermis. May be due to the elasticity and deformation of the skin, the effective penetration was found to be shorter than the total length of needles. These findings indicated that the MNs created uniform pathways and that SS was successfully delivered into the skin, which also provided the drug delivery mechanism of MNs following insertion into the skin.

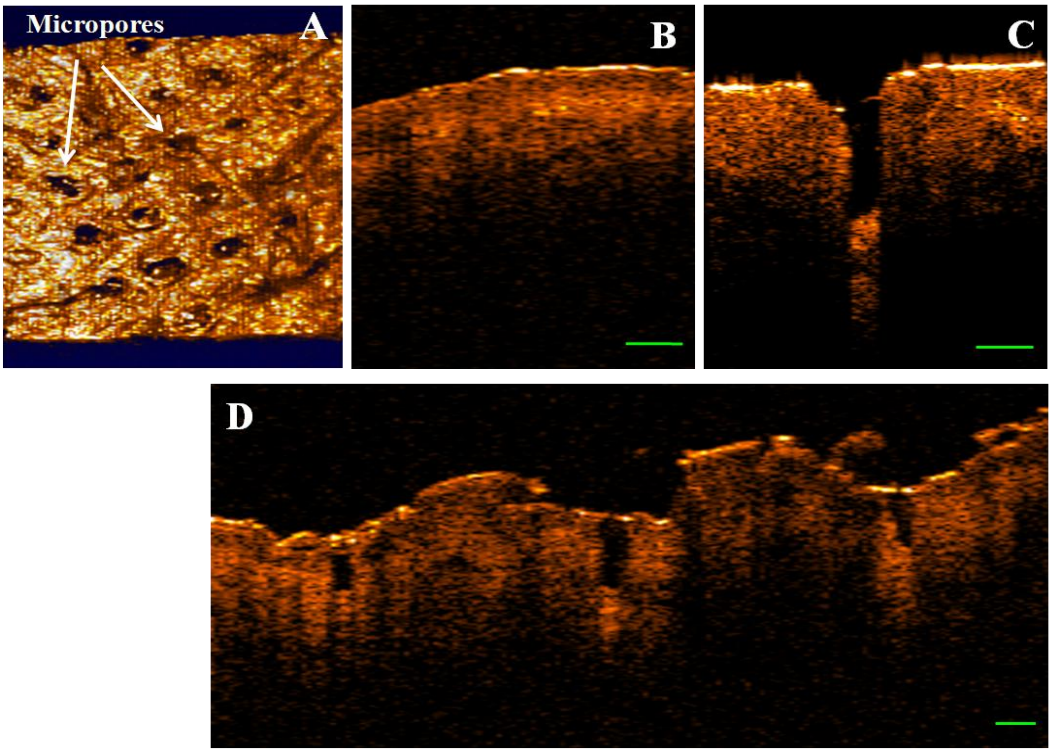

Fig. 17. Optical coherence tomography images of human cadaver skin after application of sumatriptan succinate-loaded microneedle arrays (MNs). (A) *En face* three-dimensional volumetric image of human skin after insertion of MNs. (B) Two-dimensional (2 D) image of untreated skin. (C) and (D) 2 D images of MN-treated skin. Bars = 100 μm.

2.6. *In vitro* release of SS from SS-loaded MNs

2.6.1. Methods

MNs were placed in 5 mL PBS (pH 7.4) and maintained at 32 ℃ throughout the test period, while stirring with magnetic bars at 100 rpm. At predetermined intervals, 0.5 mL of supernatant was withdrawn and replaced with an equal volume of fresh PBS. The concentration of SS was analyzed by the HPLC system described above.

2.6.2. Results

Fig. 18 shows the cumulative release of SS from dissolving MNs under perfect sink conditions. MNs dissolved rapidly and almost all the formulated SS was released within 1 h.

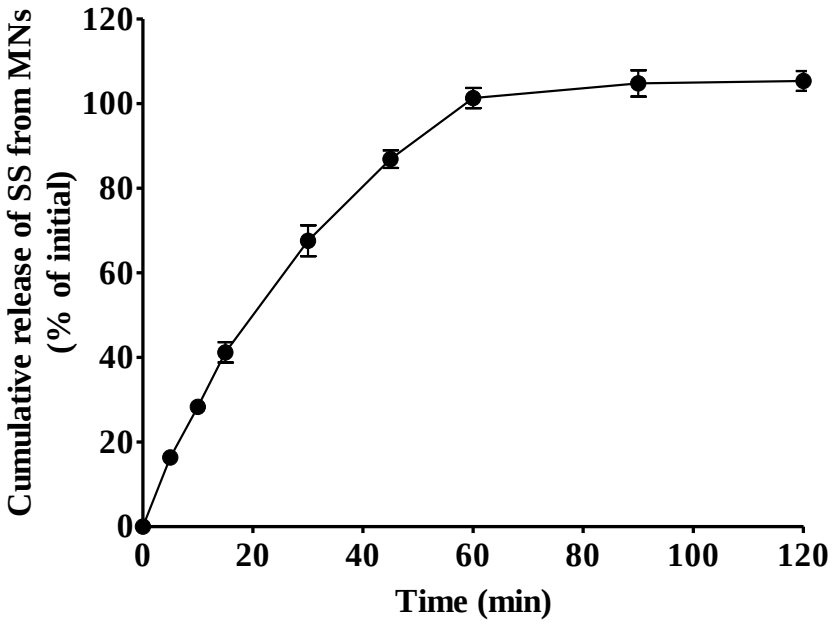

(Biological and Pharmaceutical Bulletin, Fig. 2)

Fig. 18. *In vitro* release profile of sumatriptan succinate (SS) from SS-loaded microneedle arrays (MNs) in phosphate-buffered saline (pH 7.4) maintained at 32 ℃. Results are presented as the mean ± S.E. of four experiments.

2.7. Evaluation of dissolution of SS-loaded MNs following inserting into rat skin

2.7.1. Methods

The penetration characteristics and subsequent in-skin dissolution of MNs after application into rat skin *in vivo*, were observed using OCT. Rats were anesthetized *via* an intraperitoneal injection of 40 mg/kg pentobarbital sodium and their abdominal hairs were carefully shaved using an electric clipper and a razor 24 h prior to the experiment. Just before treatment, healthy rats without signs of scratches or illness were chosen. Upon application of the MNs, the skin treated sites with inserted MNs were immediately observed using a Ganymede model OCT microscope (Thorlabs GmbH, Munich, Germany) at indicated time intervals.

2.7.2. Results

The representative cross-sectional 2 D images of the *in situ* dissolution of SS-loaded MNs following application onto rat skin were shown in Fig. 19. Needles appeared to successfully pierce into rat skin without any bending or cracking. It was appeared that needles were reduced in length by approximately 50% within 15 min, and were completely dissolved by 1 h. These findings showed that our novel MNs fabricated from sodium hyaluronate possessed self-dissolving properties, which were easily dissolved upon application onto skin.

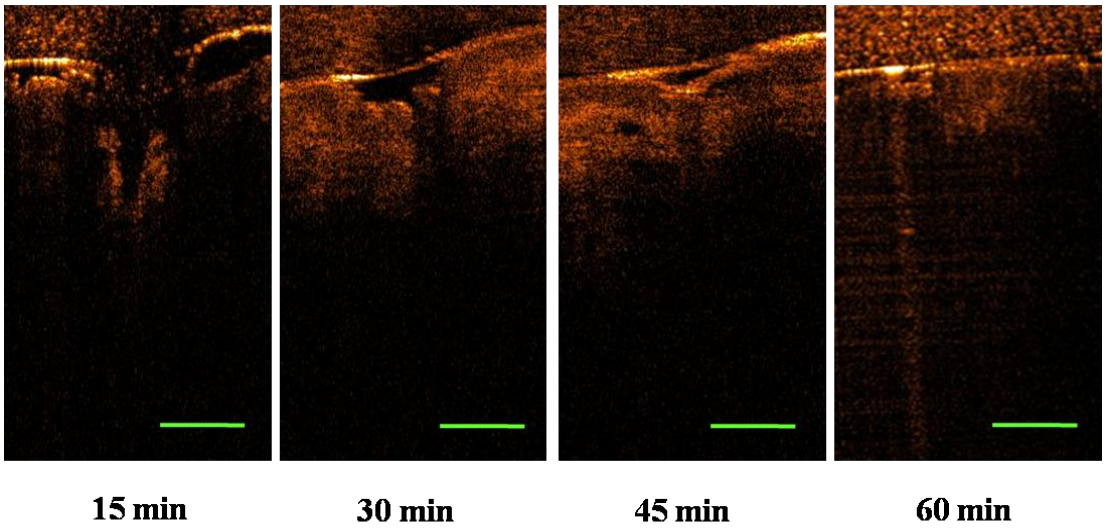

(Biological and Pharmaceutical Bulletin, Fig. 3)

Fig. 19. Representative two-dimensional optical coherence tomography images of sumatriptan succinate-loaded microneedle arrays after application onto rat skin *in vivo*. Bars = 200 μm.

2.8. Assessment of skin barrier disruption after application of SS-loaded MNs via TEWL values

2.8.1. Methods

Rats were anesthetized *via* intraperitoneal injection of 40 mg/kg pentobarbital sodium and their abdominal hair was carefully shaved using an electric clipper and a razor 24 h prior to testing. Just before treatment, healthy rats without signs of scratches or illness were chosen.

Animals were acclimatized to the ambient room temperature (25 ℃) and relative humidity (50%) for 30 min. TEWL values for rat skin were measured using a Tewameter (TM 300, Courage and Khazaka Electronic GmbH, Cologne, Germany), where a probe was applied to the skin. Three circular areas were marked on the shaved abdominal area of every rat and measured without any treatment (control group), after treatment with MNs (SS-loaded MNs group), and after tape stripping (tape stripping group). Tape stripping was achieved by applying circular adhesive cellophane tape (10 mm in diameter) to the stratum corneum surface of the skin. Each skin section was stripped sequentially with 15 pieces of adhesive tape. TEWL values represented the mean readings for 20 s before the measurements were automatically stopped. The values were recorded before and after each treatment at predetermined time intervals over a period of 24 h in all groups.

2.8.2. Results

Damaged skin shows high TEWL, while intact and healthy skin has very low TEWL values. To evaluate the skin barrier function following application of the SS-loaded MNs or tape stripping, TEWL was measured before treatment and immediately after removal of the arrays or after tape stripping at the indicated time intervals for up to 24 h. The mean TEWL of the untreated skin was 6.2 ± 0.3 g/h·m^2. As shown in Fig. 20, TEWL values significantly increased ($P < 0.001$) and peaked (47.6 ± 1.8 g/h·m^2) immediately after application of MNs and after tape stripping ($P < 0.001$, 68.8 ± 8.9 g/h·m^2), compared with the control group. However, the mean TEWL values then gradually decreased back to baseline ($P > 0.05$) within 24 h after removal of MNs. Conversely, there was no significant reduction in the mean TEWL of the tape stripping group within the experimental period; these values remained at 43.3 ± 7.6 g/h·m^2, even after 24 h, suggesting that the tape stripping caused skin damage was irreversible. These findings suggested that MNs pierced into skin successfully, caused less disruption than tape stripping, and that the MN-associated reduction in skin barrier function was reversible.

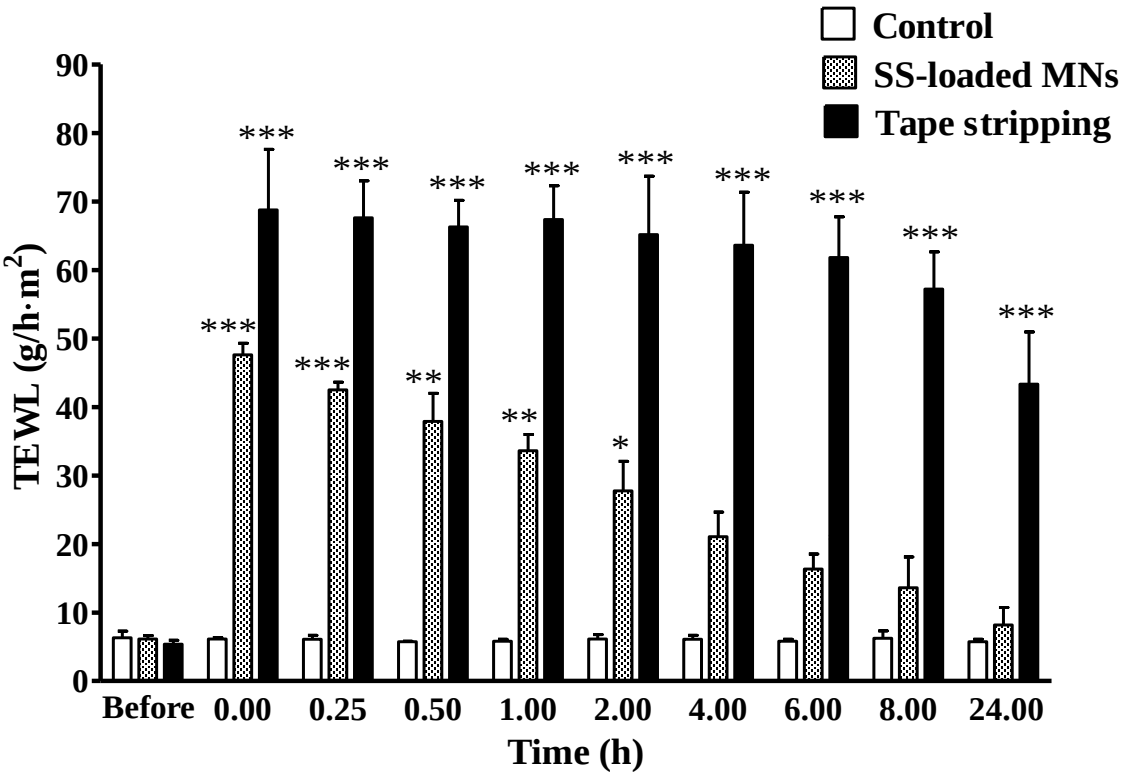

(Biological and Pharmaceutical Bulletin, Fig. 4)

Fig. 20. Transepidermal water loss (TEWL) values of rat skin before application and after removal of sumatriptan succinate-loaded microneedle arrays (SS-loaded MNs) or after tape stripping treatment at the indicated time-points. Results are presented as the mean ± S.E. of four experiments. $^{***}p < 0.001$, $^{**}p < 0.01$, $^{*}p < 0.05$, compared with the control.

2.9. Skin primary irritation after application of SS-loaded MNs to rat

2.9.1. Methods

Skin primary irritation after application of SS-loaded MNs was evaluated using a Draize method [63]. Rats were anesthetized *via* an intraperitoneal injection of 40 mg/kg pentobarbital sodium and back hairs were carefully shaved using an electric clipper and a razor 24 h prior to testing. Just before treatment, the shaved skins were closely examined to ensure their integrity, in case any damage had occurred during handling, healthy rats without signs of scratches or illness were chosen. After removal of the MNs, skin irritation was assessed by scoring the

degree of erythema and edema according to the method, as reported previously [64].

2.9.2. Results

Skin irritation after treated with MNs was recorded at 1 h, 24 h, and 72 h with the Draize scoring criteria (Fig. 21). After removal of the MNs 1 h, a certain extent erythema but no edema appeared at the treated sites and the erythema evidently lightened within 24 h. Moreover, the skin damage recovered to normal after 72 h. The Primary Irritation Index (P.I.I.) was calculated to be 2.1, indicating a moderate irritation (P.I.I. between 2.0 and 4.9, classified to moderate irritation) was induced with the SS-loaded MNs.

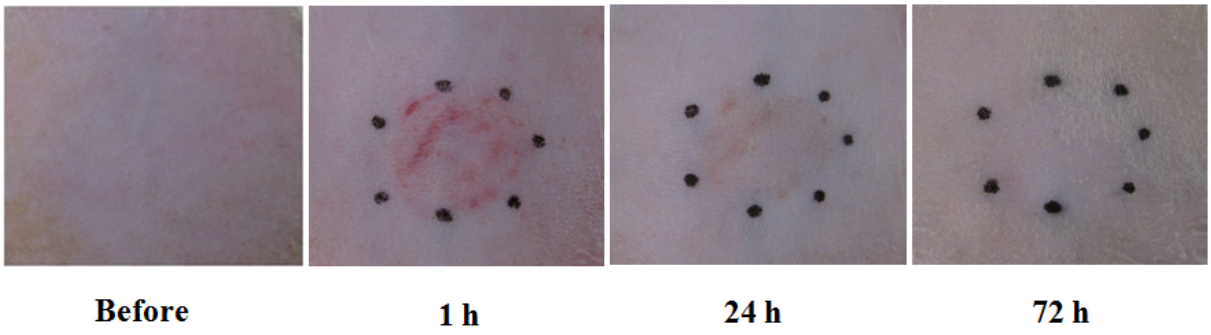

Fig. 21. Photographs of rat skin before treatment, and after removal of the sumatriptan succinate-loaded microneedle arrays at 1 h, 24 h and 72 h.

2.10. Recovery of micropores created by insertion of MNs into rat skin

2.10.1. Methods

Rats were anesthetized *via* intraperitoneal injection of 40 mg/kg pentobarbital sodium and their abdominal hair was carefully shaved using an electric clipper and a razor 24 h prior to the experiment. Just before treatment, the shaved skins were closely examined to ensure their integrity, in case any damage had occurred during handling, healthy rats without signs of scratches or illness were chosen. MNs containing 5% blue dye were then applied to the rat

skin and left in place for 4 h *in vivo*. Before and after treatment, the rat skin surface was observed over a period of 24 h using a Dermatoscope (DermaShot-Scope, Fineopto Co., Ltd., Tokyo, Japan).

2.10.2. Results

As shown in Fig. 22, micropores were created in rat skin after application of MNs. The skin surface was observed before treatment, and immediately after removal of MNs at 0, 1, 4, and 24 h. The injection sites were stained by the blue dye released from the MNs and the blue dots therefore corresponded to the needle injection sites. It was also evident from Fig. 22 that the blue color diffused quickly and had disappeared from the skin by 24 h after removal, suggesting that micropores created by MNs rapidly resealed over time. Taken together, these results indicated that the creation and recovery of micropores were consistent with the changes in TEWL values.

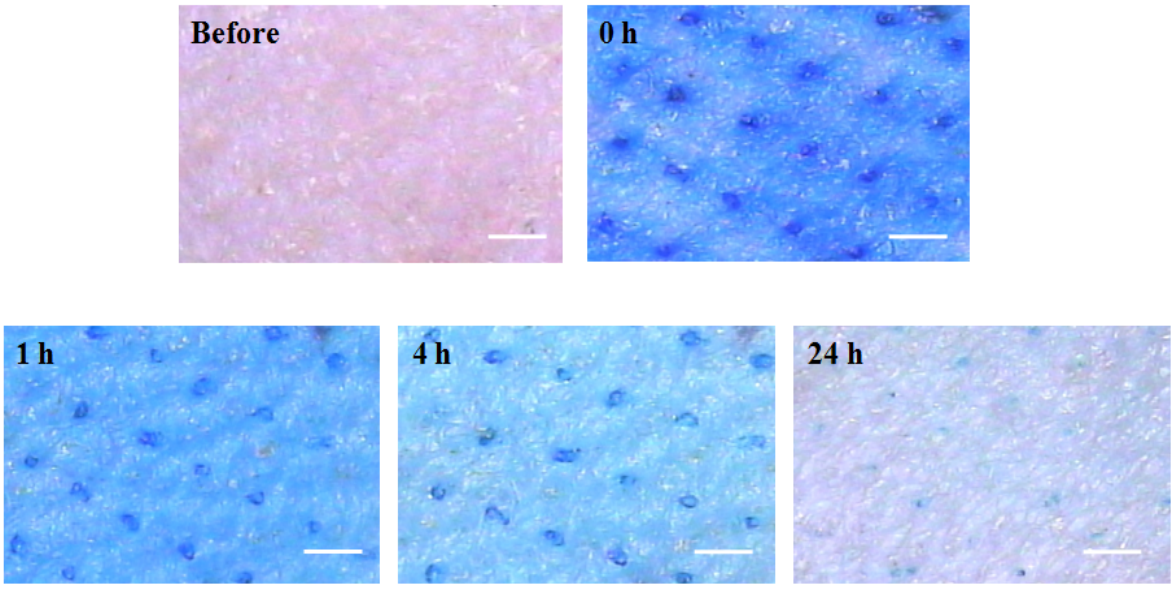

(Biological and Pharmaceutical Bulletin, Fig. 5)

Fig. 22. Microscope images of rat skin surface before treatment and after removal of 5% blue dye-contained microneedle arrays *in vivo* at the indicated time intervals. Bars = 400 μm.

2.11. *In vivo* transdermal absorption of SS from SS-loaded MNs

2.11.1. Methods

Prior to administration, rats were fasted for 12 h, with water *ad libitum*. All animals were anesthetized *via* intraperitoneal injection of 40 mg/kg pentobarbital sodium. Prior to transdermal medication, the abdominal hair was carefully shaved using an electric clipper and a razor. The following groups of animals were studied before and after drug administration [65]. (1) SS i.v. group, where SS solution (5.0 mg/kg in PBS, pH 7.4) was injected intravenously into the jugular vein using a hypodermic needle; (2) SS s.c. group, where SS solution (5.0 mg/kg) was injected subcutaneously into abdominal skin; (3) SS oral group, where SS solution (5.0 mg/kg) was administered orally using an intragastric needle; (4) MNs + SS solution group, where placebo MNs were applied onto abdominal skin and removed 5 min later, then a piece of cotton (diameter 10 mm) saturated with SS solution (5.0 mg/kg) was applied onto the treated skin site; (5) SS-loaded MNs group, where MNs containing three different amounts of SS (2.4, 5.0, and 9.6 mg/kg) were prepared and applied to abdominal skin (Fig. 23), then fixed with gum tape. Blood samples (0.5 mL) were collected from the jugular vein at 5, 15, 30, 60, 90, 120, 180, 240, 360, and 600 min after administration in all groups. Blood samples were immediately centrifuged at 12000 rpm for 5 min to separate plasma. The plasma samples were stored at -50 ℃ until analysis.

The plasma samples obtained as described above were treated and analyzed according to the following methods. Plasma samples (100 μL) were mixed with 1 mL acetonitrile and vortexed for 1 min to precipitate protein. After centrifugation at 12000 rpm for 5 min, the clear supernatant layer was collected and evaporated using a centrifugal concentrator (VC-36N, TAITEC Co., Ltd., Saitama, Japan) to remove organic solvents. The dried residue was reconstituted with 150 μL PBS (pH 7.4) and centrifuged before being injected into the HPLC system described above.

C_{max} and T_{max} were determined directly from the individual plasma concentration-time

profile. AUC for 0→10 h was calculated by the linear trapezoidal rule method. Absolute BA was calculated according to the following equation:

$$BA\ (\%) = (AUC_{MN} \times Dose_{i.v.})/(AUC_{i.v.} \times Dose_{MN}) \times 100$$

Where AUC_{MN} and $AUC_{i.v.}$ indicated the AUCs after applying SS-loaded MNs and after i.v. injection of SS, respectively. The BA for other administration routes was calculated using the same method.

All statistical analyses were performed using GraphPad Prism software (GraphPad Software Inc., San Diego, CA, U.S.A.). Student's unpaired *t*-tests were used for comparisons between groups. Results are presented as mean values ± S.E. In all cases, $P < 0.05$ was considered to be statistically significant.

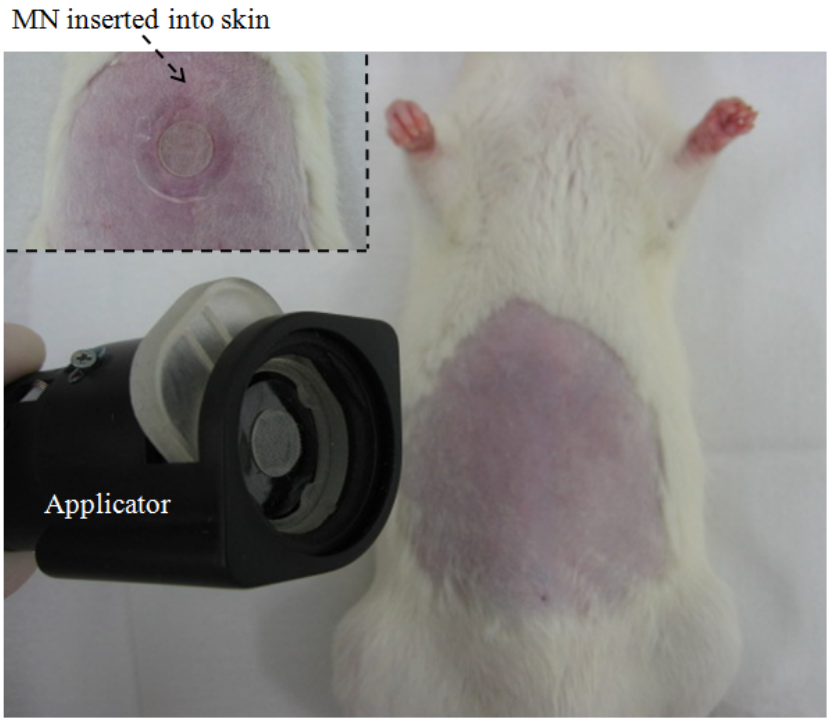

Fig. 23. Sumatriptan succinate-loaded mironeedle array (MN) was applied to the shaved rat skin with an applicator in the *in vivo* absorption study.

2.11.2. Results

As shown in Fig. 24A, SS rapidly disappeared from the blood circulation after its i.v. injection. After oral administration, SS was rapidly absorbed from the gastrointestinal tract with a C_{max} of 0.2 ± 0.1 μg/mL at a T_{max} of 26.3 ± 3.8 min. In contrast, there was only a small spike in plasma SS concentration in the MNs + SS solution group, compared with the levels achieved using SS-loaded MNs and s.c. injection (Fig. 24B). A significant and dose-dependent increase in plasma SS concentration was observed after treatment with SS-loaded MNs. The peak plasma SS levels were reached within an hour and ranged from 1.0 ± 0.7 to 4.0 ± 0.5 μg/mL as the dose increased from 2.4 to 9.6 mg/kg.

The pharmacokinetic parameters after administration of SS after administration by a range of methods were calculated and summarized in Table 2. There were significant differences between the BA ($P < 0.001$) values after transdermal administration of SS-loaded MNs *vs.* oral administration. The absolute BA of SS after treatment with different doses of SS-loaded MNs ranged from 87.6 ± 14.3% to 90.4 ± 10.3%. In addition, very low $AUC_{0\rightarrow 10h}$ (2.6 ± 0.6 μg·min/mL) and BA (0.8 ± 0.3%) values were achieved in the MNs + SS solution group. As we expected, SS was sufficiently absorbed from skin into the systemic circulation after treatment with SS-loaded MNs, and the use of MNs dramatically improved the BA of SS, as compared with oral administration. Additionally, the pharmacokinetic parameters of the SS-loaded MNs were similar to those observed after s.c. injection. These findings indicated that the absorption and delivery of SS administered using SS-loaded MNs were comparable to those achieved by s.c. injection.

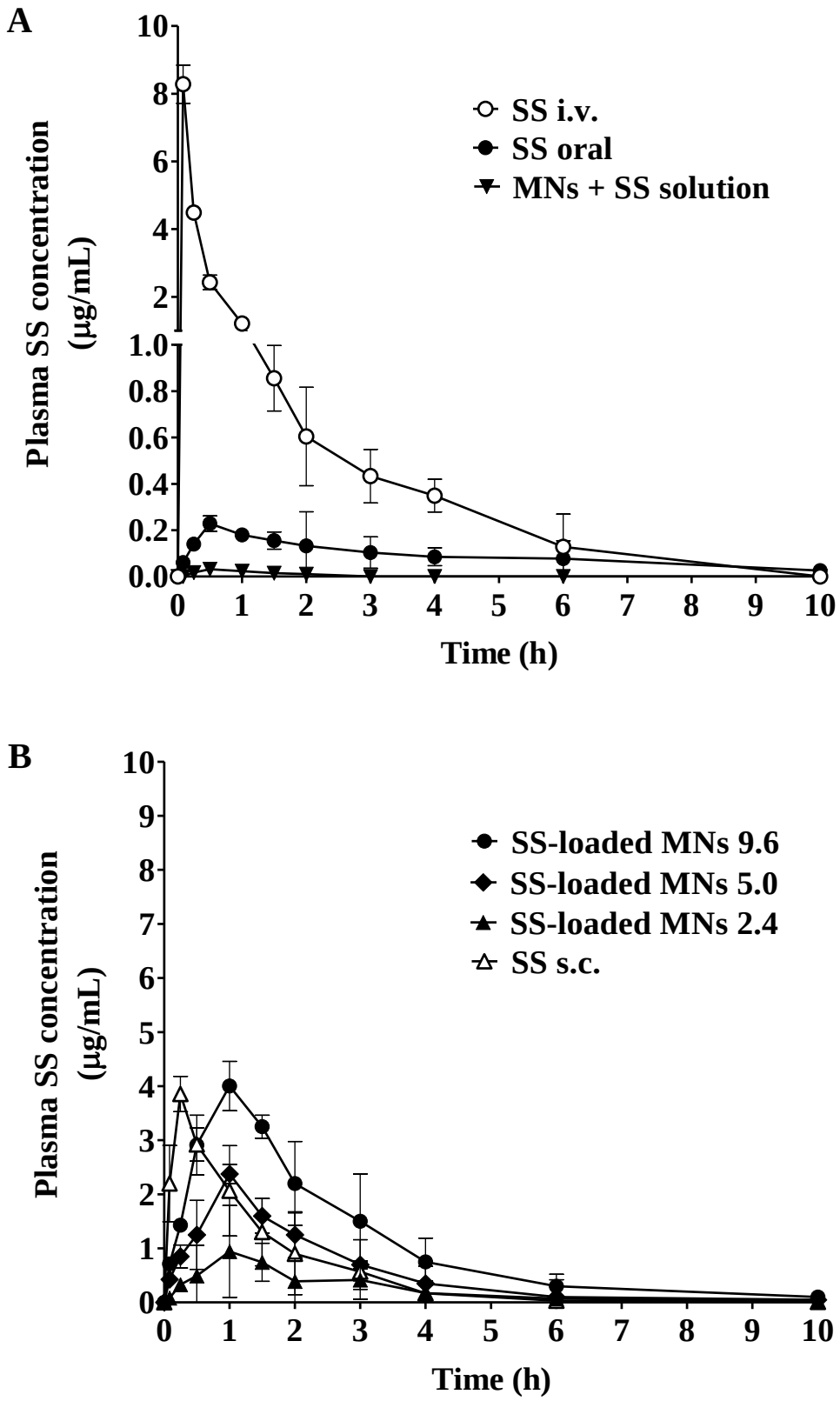

(Biological and Pharmaceutical Bulletin, Fig. 6)

Fig. 24. Plasma concentration-time profiles of sumatriptan succinate (SS) after intravenous (i.v.), oral, subcutaneous (s.c.) and transdermal administration. Results are presented as the mean ± S.E. of at least four experiments.

Table 2. Pharmacokinetic parameters of sumatriptan succinate (SS) after intravenous (i.v.), oral, subcutaneous (s.c.) and transdermal administration in rats.

Groups	Dose (mg/kg)	C_{max} (μg/mL)	T_{max} (min)	$AUC_{0\rightarrow10h}$ (μg·min/mL)	BA (%)
SS i.v.	5.0	-	-	328.5 ± 25.7	-
SS oral	5.0	0.2 ± 0.1	26.3 ± 3.8	67.3 ± 5.5	20.5 ± 3.8
SS s.c.	5.0	3.9 ± 0.3	15.0 ± 0.0	306.4 ± 9.5	93.3 ± 7.6
SS-loaded MNs 2.4	2.4	1.0 ± 0.7	75.0 ± 8.7	138.1 ± 24.0	87.6 ± 14.3***
SS-loaded MNs 5.0	5.0	2.4 ± 0.2	67.5 ± 7.5	295.1 ± 3.6	89.8 ± 2.1***
SS-loaded MNs 9.6	9.6	4.0 ± 0.5	52.5 ± 6.7	570.3 ± 18.9	90.4 ± 10.3***
MNs + SS solution	5.0	0.03 ± 0.02	22.5 ± 4.3	2.6 ± 0.6	0.8 ± 0.3

Results are presented as the mean ± S.E. of at least four experiments. *** $p < 0.001$, compared with oral administration. (Biological and Pharmaceutical Bulletin, Table 1)

2.12. Discussion

In the present study, sodium hyaluronate was used to produce a self-dissolving MN for enhancing the transdermal delivery of SS. As sodium hyaluronate is a skin tissue component, it is considered safe for this biomedical application. It was apparent that MNs had advantages over the traditional passive patch system, since they could overcome the stratum corneum barrier by inserting into the skin and could effectively improve the transdermal delivery of SS, these findings suggested that the novel MN-mediated system was the optimal method for transdermal SS delivery.

In order to improve the transdermal delivery of SS from the SS-loaded MNs, we evaluated the effect of needle length, thickness, density and penetration enhancers on the skin permeation amount of SS. It was found that MNs having different lengths affected transdermal delivery of SS, with 800 μm long MNs delivering more SS across skin compared to that of 500 μm. This finding was consistent with reports by Oh *et al*. who estimated the influence of needle length on the skin permeation of calcein, and showed that 500 μm MNs significantly increased drug delivery compared with that of 200 μm MNs [66]. However, as shown in Fig. 10A, there was approximately 1.1 mg/cm^2 SS was detected in the receptor compartment within 4 h, which was too low to achieve the therapeutic action compared with the case of Zecuity® (NuPathe Inc, Conshohocken, PA, U.S.A.), an iontophoretic delivery system containing SS for the acute treatment of migraine, which contains 86 mg sumatriptan (base) and is able to deliver 6.5 mg sumatriptan (base) over 4 h.

To further improve the skin permeation amount of SS, we tried to enhance the drug loading of MNs by increasing the thickness of needles. Indeed, the SS loading was improved from 9.8 to 11.2 mg/cm^2. However, Fig. 11A indicated no significant differences of the permeation profiles between the usual MNs and the thick MNs. This may be plausible that the saturation of the SS aqueous solution we used to fabricate the SS-loaded MNs, therefore the transport becomes independent of concentration. Afterwards, it was also found that the delivery of SS did not increase by addition of enhancers, which may be explained that after inserting MNs into skin, the water soluble needles rapidly dissolved upon touching the skin interstitial fluid and, hence, it was difficult to bring the enhancers' superiority to play. On the other hand, the enhancers may be more useful for the needle free transdermal preparations, by using which could raise the delivery of model drugs through the skin barrier.

Cumulative permeated amount of SS was found to significantly increase with increased number of needles. Assuming each MN created perfectly circular hole of exactly the same dimensions of its base diameter, this would mean that the surface hole area induced by usual

and high density MN was calculated to be about 3.5 $\times 10^6$ μm^2 and 4.8 $\times 10^6$ μm^2, respectively. By increasing the numbers of needles per array, resulting in a 1.4-fold increase in the total hole area. Consequently, it was possible that the enhancement in SS penetration observed may be largely due to an increase in the surface area of the MN-induced holes. These findings were well consistent with the previous studies [43,46]. It was also evident from Fig. 13A that the high density MNs delivered around 2.2 mg/cm^2 SS within 4 h, which equaled to 1.6 mg/cm^2 sumatriptan base (*MW* of SS was 413.5 Da, *MW* of sumatriptan base was 295.2 Da) was able to delivered into the skin. Based on the market available s.c. injection formulation Imitrex® (GlaxoSmithKline, Brentford, Middlesex, UK) of sumatriptan for the treatment of migraine, for single dose, 6 mg is needed in the U.S.A., whereas in Japan 3 mg is set basing on the similar analgesic effect. With these findings in mind, we concluded that for the transdermal delivery of sumatriptan, approximately 3.5 mg is enough for anti-migraine therapy in Japan, in contrast to 6.5 mg of Zecuity® in U.S.A. In addition, for the MNs with the length of 800 μm, the maximum diameter suitable for clinical application is 2 cm, which means the maximum area of each circular array is limited to 3.14 cm^2. In the present study, it was found that about 1.6 mg/cm^2 sumatriptan was delivered with the diameter of 1 cm, assuming that increased the diameter to 2 cm, approximately 5.0 mg sumatriptan would be delivered into the skin, which considerably exceeds our target 3.5 mg. Therefore, although further practical verifications are needed, our MNs containing 11.0 mg/cm^2 SS with the circular diameter of 2 cm is feasible to deliver therapeutic dose of SS to migraine patients, and was chosen for the further *in vitro* and *in vivo* characterizations studies.

Due to the hydrophilicity of sodium hyaluronate, our fabricated MNs might easily absorb moisture under conditions of high humidity, which could affect needle morphology and/or strength. We therefore evaluated the effect of hygroscopy on the mechanical strength of SS-loaded MNs. It was found that the MNs maintained their skin piercing capability for up to 30 min after being placed at a high relative humidity of 75%. Moreover, the structure of MNs

did not change during the 24 h experimental period. These findings indicated the feasibility of practical application of these MNs. Our sodium hyaluronate based MNs therefore had an advantage over previously reported dissolvable MNs. For example, MNs fabricated from galactose by Donnelly *et al*. rapidly deformed in conditions exceeding humidity of 43%, and completely dissolved within 1 h at a relative humidity of 75% [47].

OCT is a non-destructive optical imaging technique which allows acquisition of 2 D or three-dimensional (3 D) image data *in situ* and in real time, up to a depth of 2 mm below the surface of the tissue [67,68]. Recently, OCT has been as a valuable tool to evaluate the penetration characteristics, and subsequent in-skin dissolution kinetics of MNs after application onto skin [69,70]. We chose OCT, rather than traditional histological sectioning and staining, to visualize drug pathways in real time after the removal of MNs, thus avoiding skin damage by freezing, which could result in an altered skin structure. It was found that distinct uniform micropores were created *en face*, confirming that the stratum corneum had been breached. In addition, 2 D images indicated that the MNs had successfully penetrated the epidermis and extended into the papillary dermis. The results further proved that even in the case of high drug loading, these sodium hyaluronate-fabricated MNs, with a tapered cone-shape geometry, possessed sufficient mechanical strength to puncture the human skin, and that a length of 800 μm was sufficiently long to deliver SS into the upper dermis.

Compared with silicon-, metal- or glass-fabricated MNs, our novel MNs choosing sodium hyaluronate as the basal materials were biocompatible. We observed that microneedles were totally dissolved after *in vivo* application onto rat skin by 1 h. It was also noted that almost all of the formulated SS was released from the MNs within 1 h *in vitro*, indicating that these MNs were speedily and completely dissolved in aqueous solution. These findings suggested that SS was rapidly released from the arrays both *in vitro* and *in vivo*.

To evaluate the integrity of the stratum corneum barrier and skin permeability, TEWL values were measured after application of MNs and after tape stripping treatment [71-73]. We

found that although TEWL immediately increased after application of MNs, the values were lower than those observed after tape stripping treatment. Furthermore, TEWL gradually recovered back to baseline levels within the experimental period after MN treatment, implying that the micropores created by MNs were subsequently closed. In contrast, no significant recovery in TEWL was seen after tape stripping. These findings corroborated those of previous reports [74]. It is well known that an increase in TEWL reflects skin disruption and enhanced skin permeability. These findings confirmed that the MNs effectively pierced the skin, consistent with the OCT data.

It was found that moderate irritations were emerged along with the high density SS-loaded MNs, which was slightly higher than that of placebo usual MNs (P.I.I. was 1.7, classified to slight irritations) [64]. It may be plausible that increased number of needles was in parallel to increase the number of pores per unit area, thus, resulting in relatively higher skin damage, as confirmed in the skin permeation experiments as mentioned above.

To vividly observe resealing of micropores created after application of MNs, we recorded the surface of the treated skin. This revealed that the small pores rapidly resealed over time, and had almost entirely disappeared within 24 h. This finding was highly consistent with the results obtained from TEWL measurement. The increases in TEWL values corresponded to pore creation, while decreases in TEWL could be attributed to effective pore resealing. Zhou *et al*. previously reported that MNs induced much less skin damage than a 25-G hypodermic needle [74]. Therefore, these results demonstrated that skin puncture by the dissolving MNs caused only slight skin damage, which was reversible *in vivo*.

Various transdermal systems were developed to achieve SS delivery *via* the skin, instead of more traditional formulations [15-19,75,76]. In addition to *in vitro* and preclinical studies, Pierce *et al*. [19] reported an iontophoretic transdermal technology for the acute treatment of migraine, where the T_{max} was approximately 2 h and serum SS concentration was maintained at 20 ng/mL for 4 h in humans, indicating effective SS delivery. However, this delivery

system had disadvantages, including local reactions at the application site that could result in pruritus or pain [60,61]. Compared with these previous studies, the present study demonstrated that SS could be delivered into the systemic circulation effectively and painlessly using SS-loaded MNs fabricated from highly biocompatible sodium hyaluronate, thus resulting in good patient compliance. The transdermal absorption of SS after application of the MNs was almost equivalent to that observed after s.c. injection. High SS absolute BA (approximately 90%) was obtained after the application of SS-loaded MNs, which was much higher than that produced by oral administration. These findings suggested that this novel MN system could improve the transdermal delivery of SS effectively. Additionally, compared with s.c. injection, the slightly prolonged T_{max} and low C_{max} values seen following MN application may be due to the time required for the SS-loaded MNs to dissolve, providing a more sustained delivery of SS to the systemic circulation, in contrast to the rapid diffusion of SS following s.c. injection.

In addition, it was also demonstrated that only a marginal plasma concentration was achieved by application of SS solution to MNs pretreated skin. This may reflect the rapid closure of the small pores created by MNs, as confirmed by the TEWL and micropore recovery experiments above. Therefore, the delivery of SS gradually reduced over time and most of the SS was trapped in the stratum corneum. However, further studies are required to clarify this finding.

We observed that no significant differences in the pharmacokinetic characteristics of the SS-loaded MN group and the s.c. injection group using the same doses of SS, suggesting that SS-loaded MNs delivered similar amounts of SS as s.c. injection. These findings demonstrated that the novel sodium hyaluronate MN delivery system was an excellent alternative candidate for delivering SS to migraine patients, while avoiding the pain associated with use of hypodermic needles.

COMPARISONS BETWEEN WATER EMULSION PATCH AND SELF-DISSOLVING MN

In this study, both the Nikasol patch and sodium hyaluronate MN were successfully developed for increasing transdermal delivery of SS into systemic circulation.

Merits of the patch system were tiny or negligible skin irritation, easy to self-administration without external application devices. However, even it was feasible in delivering therapeutic amount of SS to the skin, the large size was inconvenient in practical application. On the other hand, the transdermal patch system will be more effective for the compounds with hydrophobicity, good compatibility with adhesive, or when parenteral administration is necessary.

MN was able to pierce the skin barrier, thus delivering contained SS to the skin at efficient level even in a small size. Moderate skin irritation was induced after application of SS-loaded MN, however, the skin damage recovered to normal within 24 h. Moreover, the novel MN choosing sodium hyaluronate as basal material possessed high biocompatibility and were able to dissolve upon application to the skin. Even though in case of multiple administrations, less pain and lower side effects including skin reactions will be caused when compared with hypodermic needles. MN has high potential to efficiently deliver a variety of compounds into skin, especially for those which are difficult to pass through the skin such as protein or drugs have high hydrophilicity. In addition, MN associated rapid onset of action, which is very useful in anti-migraine treatment, in contrast to the prolonged delivery of SS following the patch system.

Therefore, based on these findings, for transdermal delivery of SS, a high dose, high hydrophilicity, and low molecular weight drug, the novel self-dissolving MN seems to be a more effective method in clinical setting.

CONCLUSIONS

Chapter 1:

1) Nikasol was found to be a much more excellent adhesive than HGA in increasing permeability and absorption of SS cross the skin.
2) Compared with oral administration, the Nikasol patch achieved a higher BA and consistent plasma concentration over an extended period of time.

Chapter 2:

1) Skin permeation of SS from the sodium hyaluronate-fabricated SS-loaded MNs could be modulated by controlling needle length and density to achieve the clinical therapy requirements.
2) The novel self-dissolving SS-loaded MNs were strong enough to uniformly penetrate the skin without breakage, and possessed suitable hygroscopy, drug release profiles and dissolution properties.
3) The skin disruption caused by MNs was reversible, and the micro pores created by MNs recovered within 24 h after application.
4) The delivery of SS achieved by MNs was almost equivalent to that observed after subcutaneous injection, and was considerably higher than that associated with oral administration.

To sum up, both the Nikasol patches and the sodium hyaluronate MNs are useful alternative approaches for increasing transdermal delivery of SS without serious skin damage. Further, the novel MNs are a much more effective formulation in the clinical application.

ACKNOWLEDGMENTS

I would like to express my heartfelt gratitude to:

Professor Akira Yamamoto, my distinguished supervisor, for his constant guidance, patience, tolerance and genuine enthusiasm throughout my academic years. It has been a great honor and joy to study under his guidance and supervision;

Associate Professor Toshiyasu Sakane, Dr. Hidemasa Katsumi, Dr. Kosuke Kusamori, Dr. Kunio Yoneto, Dr. Fumio Kamiyama and Dr. Ying-shu Quan, for providing good work facilities, kind instruction and valuable suggestion in this research;

Ms. Yutaro Tanaka, Ms. Yong-ri Jin and all members of the Department of Biopharmaceutics, Kyoto Pharmaceutical University, for their kind supports, collaboration and friendly assistance;

Last, but not least, my husband, daughter, parents, brother, sister-in-law and friends, for their understanding, constant support and boundless love. In particular, my mother and mother-in-law for their great help in taking care of my daughter. My beloved family gives me encouragement and driving force to complete the doctoral degree.

REFERENCES

[1] D.K. Arulmozhi, A. Veeranjaneyulu, S.L. Bodhankar. Migraine: Current concepts and emerging therapies. *Vascul. Pharmacol.*, 43, 176–187 (2005).

[2] J. Olesen, M. Ashina. Emerging migraine treatments and drug targets. *Trends Pharmacol. Sci.*, 32, 352–359 (2011).

[3] K.M. Al Azzam, B. Saad, C.Y. Tat, I. Mat, H.Y. Aboul-Enein. Stability-indicating micellar electrokinetic chromatography method for the analysis of sumatriptan succinate in pharmaceutical formulations. *J. Pharm. Biomed. Anal.*, 56, 937–943 (2011).

[4] S.S. Jhee, T. Shiovitz, A.W. Crawford, N.R. Cutler. Pharmacokinetics and pharmacodynamics of the triptan antimigraine agents: a comparative review. *Clin Pharmacokinet.*, 40, 189–205 (2001).

[5] A. Kovács, L.G. Hársing, G. Szénási. Vasoconstrictor 5-HT receptors in the smooth muscle of the rat middlecerebral artery. *Eur. J. Pharmacol.*, 689, 160–164 (2012).

[6] P.W. Major, H.S.I. Grubisa, N.M.R. Thie. Triptans for treatment of acute pediatric migraine: a systematic literature review. *Pediatr Neurol*, 29, 425–429 (2003).

[7] P. Tfelt-Hansen. Efficacy and adverse events of subcutaneous, oral, and intranasal sumatriptan used for migraine treatment: a systematic review based on number needed to treat. *Cephalalgia*, 18, 532–538 (1998).

[8] L.F. Lacey, E.K. Hussey, P.A. Fowler. Single dose pharmacokinetics of sumatriptan in healthy volunteers. *Eur. J. Clin. Pharmacol.*, 47, 543–548 (1995).

[9] M.D. Ferrari, K.I. Roon, R.B. Lipton, P.J. Goadsby. Oral triptans (serotonin 5-$HT_{1B/1D}$ agonists) in acute migraine treatment: a meta-analysis of 53 trials. *Lancet*, 358, 1668–1675 (2001).

[10] C.M. Dixon, G.R. Park, M.H. Tarbit. Characterization of the enzyme responsible for the metabolism of sumatriptan in human liver. *Biochem. Pharmacol.*, 47, 1253–1257

(1994).

[11] J.E. Hardebo, C. Dahlöf. Sumatriptan nasal spray (20 mg/dose) in the acute treatment of cluster headache. *Cephalalgia*, 18, 487–489 (1998).

[12] R.E. Cull, W.H. Price, A. Dunbar. The efficacy of subcutaneous sumatriptan in the treatment of recurrence of migraine headache. *J. Neurol. Neurosurg. Psychiatr.*, 62, 490–495 (1997).

[13] A. Alexander, S. Dwivedi, Ajazuddin, T.K. Giri, S. Saraf, S. Saraf, D.K. Tripathi. Approaches for breaking the barriers of drug permeation through transdermal drug delivery. *J. Control. Release*, 164, 26–40 (2012).

[14] K. Saioha, B. Yadav, B. Sharma. Transdermal patch: a discrete dosage form. *J. Curr. Pharm. Res.*, 3, 98–108 (2011).

[15] M.W. Pierce. Transdermal delivery of sumatriptan for the treatment of acute migraine. *Neurotherapeutics*, 7, 159–163 (2010).

[16] A. Femenía-Font, C. Balaguer-Fernández, V. Merino, V. Rodilla, A. López-Castellano. Effect of chemical enhancers on the *in vitro* percutaneous absorption of sumatriptan succinate. *Eur. J. Pharm. Biopharm.*, 61, 50–55 (2005).

[17] S.R. Patel, H. Zhong, A. Sharma, Y.N. Kalia. *In vitro* and *in vivo* evaluation of the transdermal iontophoretic delivery of sumatriptan succinate. *Eur. J. Pharm. Biopharm.*, 66, 296–301 (2007).

[18] C. Balaguer-Fernández, A. Femenía-Font, S.D. Rio-Sancho, V. Merino, A. López-Castellano. Sumatriptan succinate transdermal delivery systems for the treatment of migraine. *J. Pharm. Sci.*, 97, 2102–2109 (2008).

[19] M. Pierce, T. Marbury, C. O'Neill, S. Siegel, W. Du, T. Sebree. Zelrix^{TM}: a novel transdermal formulation of sumatriptan. *Headache*, 49, 817–825 (2009).

[20] S.J. Siegel, C. O'Neill, L.M. Dubé, P. Kaldeway, R. Morris, D. Jackson, T. Sebree. A unique iontophoretic patch for optimal transdermal delivery of sumatriptan. *Pharm. Res.*,

24, 1919–1926 (2007).

[21] Y.-C. Ah, J.-K. Choi, Y.-K. Choi, H.-M. Ki, J.-H. Bae. A novel transdermal patch incorporating meloxicam: *in vitro* and *in vivo* characterization. *Int. J. Pharm.*, 385, 12–19 (2010).

[22] C.-W. Park, D.-D. Son, J.-Y. Kim, T.-O. Oh, J.-M. Ha, Y.-S. Rhee, E.-S. Park. Investigation of formulation factors affecting *in vitro* and *in vivo* characteristics of a galantamine transdermal system. *Int. J. Pharm.*, 436, 32–40 (2012).

[23] A.M. Wokovich, S. Prodduturi, W.H. Doub, A.S. Hussain, L.F. Buhse. Transdermal drug delivery system (TDDS) adhesion as a critical safety, efficacy and quality attribute. *Eur. J. Pharm. Biopharm.*, 64, 1–8 (2006).

[24] H.S. Tan, W.R. Pfister. Pressure-sensitive adhesives for transdermal drug delivery systems. *Pharm. Sci. Tech. Today.*, 2, 60–69 (1999).

[25] K. Kusamori, H. Katsumi, M. Abe, A. Ueda, R. Sakai, R. Hayashi, Y. Hirai, Y.-S. Quan, F. Kamiyama, T. Sakane, A. Yamamoto. Development of a novel transdermal patch of alendronate, a nitrogen-containing bisphosphonate, for the treatment of osteoporosis. *J. Bone Miner. Res.*, 25, 2582–2591 (2010).

[26] Y.C. Kim, J.H. Park, M.R. Prausnitz. Microneedle for drug and vaccine delivery. *Adv. Drug Deliv. Rev.*, 64, 1547–1568 (2012).

[27] V. Sachdeva, A.K. Banga. Microneedles and their applications. *Recent Pat. Drug Deliv. Formul.*, 5, 95–132 (2011).

[28] T.M. Tuan-Mahmood, M.T. McCrudden, B.M. Torrisi, E. McAlister, M.J. Garland, T.R. Singh, R.F. Donnely. Microneedles for intradermal and transdermal drug delivery. *Eur. J. Pharm. Biopharm.*, 50, 623–637 (2013).

[29] H.S. Gill, D.D. Denson, B.A. Burris, M.R. Prausnitz, Effect of microneedle design on pain in human volunteers. *Clin. J. Pain*, 24, 585–594 (2008).

[30] M.I. Haq, E. Smith, D.N. John, M. Kalavala, C. Edwards, A. Anstey, A. Morrissey, J.C.

Birchall. Clinical administration of microneedles: skin puncture, pain and sensation. *Biomed Microdevices*, 11, 35–47 (2009).

[31] Y. Zhang, K. Brown, K. Siebenaler, A. Determan, D. Dohmeier, K. Hansen. Development of lidocaine-coated microneedle product for rapid, safe, and prolonged local analgesic action. *Pharm. Res.*, 29, 170–177 (2012).

[32] S. Liu, M.N. Jin, Y.S. Quan, F. Kamiyama, H. Katsumi, T. Sakane, A. Yamamoto. The development and characteristics of novel microneedle arrays fabricated from hyaluronic acid, and their application in the transdermal delivery of insulin. *J. Control. Release*, 161, 933–941 (2012).

[33] M. Pearton, V. Saller, S.A. Coulman, C. Gateley, A.V. Anstey, V. Zarnitsyn, J. C. Birchall, Microneedle delivery of plasmid DNA to living human skin: Formulation coating, skin insertion and gene expression. *J. Control. Release*, 160, 561–569 (2012).

[34] D. Yin, W. Liang, S. Xing, Z. Gao, W. Zhang, Z. Guo, S. Gao. Hepatitis B DNA vaccine-polycation nano-complexes enhancing immune response by percutaneous administration with microneedle. *Biol. Pharm. Bull.*, 36, 1283–1291 (2013).

[35] Y.C. Kim, D.G. Yoo, R.W. Compans, S.M. Kang, M.R. Prausnitz. Cross-protection by co-immunization with influenza hemagglutinin DNA and inactivated virus vaccine using coated microneedles. *J. Control. Release*, 172, 579–588 (2013).

[36] Y. Xie, B. Xu, Y. Gao, Controlled transdermal delivery of model drug compounds by MEMS microneedle array. *Nanomedicine*, 1, 184–190 (2005).

[37] G. Yan, K.S. Warner, J. Zhang, S. Sharma, B.K. Gale, Evaluation needle length and density of microneedle arrays in the pretreatment of skin for transdermal drug delivery. *Int. J. Pharm.*, 391, 7–12 (2010).

[38] Y. Qiu, Y. Gao, K. Hu, F. Li. Enhancement of skin permeation of docetaxel: A novel approach combing microneedle and elastic liposomes. *J. Control. Release*, 129, 144–150 (2008).

[39] H. Chen, H. Zhu, J. Zheng, D. Mou, J. Wan, J. Zhang, T. Shi, Y. Zhao, H. Xu, X. Yang, Iontophoresis-driven penetration of nanovesicles through microneedle induced skin microchannels for enhancing transdermal delivery of insulin. *J. Control. Release*, 139, 63–72 (2009).

[40] W. Martanto, J.S. Moore, O. Kashlan, R. Kamath, P.M. Wang, J.M. O'Neal, M.R. Prausnitz. Microinfusion using hollow microneedles. *Pharm. Res.*, 23, 104–113 (2006).

[41] J.H. Park, M.G. Allen, M.R. Prausnitz. Biodegradable polymer microneedles: Fabrication, mechanics and transdermal drug delivery. *J. Control. Release*, 104, 51–66 (2005).

[42] M.T.C. McCrudden, A.Z. Alkilani, C.M. McCrudden, E. McAlister, H.O. McCarthy, A.D. Woolfson, R.F. Donnelly. Design a physicochemical characterization of novel dissolving polymeric microneedle arrays for transdermal delivery of high dose, low molecular weight drugs. *J. Control. Release*, 180, 71–80 (2014).

[43] Y.A. Gomaa, M.J. Garland, F. Mclnnes, L.K. El-Khordagui, C. Wilson, R.F. Donnelly. Laser-engineered dissolving microneedles for active transdermal delivery of nadroparin calcium. *Eur. J. Pharm. Biopharm.*, 82, 299–307 (2012).

[44] C.Y. Jin, M.H. Han, S.S. Lee, Y.H. Choi, Mass producible and biocompatible microneedle patch and functional verification of its usefulness for transdermal drug delivery. *Biomed. Microdev.*, 11, 1195–1203 (2009).

[45] C.S. Kolli, A.K. Banga. Characterization of solid maltose microneedles and their use for transdermal delivery. *Pharm. Res.*, 25, 104–113 (2008).

[46] G. Li, A. Badkar, S. Nema, C.S. Kolli, A.K. Banga. *In vitro* transdermal delivery of therapeutic antibodies using maltose microneedles. *Int. J. Pharm.*, 368, 109–115 (2009).

[47] R.F. Donnelly, D.I.J. Morrow, T.R.R. Singh, K. Migalska, P.A. McCarron, C. O'Mahony, A.D. Woolfson. Processing difficulties and instability of carbohydrate microneedle arrays. *Drug. Dev. Ind. Pharm.*, 35, 1242–1254 (2009).

[48] Y. Ito, E. Hagiwara, A. Saeki, N. Sugioka, K. Takada, Feasibility of microneedles for percutaneous absorption of insulin. *Eur. J. Pharm. Sci.*, 29, 82–88 (2006).

[49] J.W. Lee, J.H. Park, M.R. Prausnitz, Dissolving microneedles for transdermal drug delivery. *Biomaterials*, 29, 2113–2124 (2008).

[50] K. Migalska, D.I.J. Morrow, M.J. Garland, R. Thakur, A.D. Woolfson, R.F. Donnelly. Laser-engineered dissolving microneedle arrays for transdermal macromolecular drug delivery. *Pharm. Res.*, 28, 1919–1930 (2011).

[51] M. Takaya, T. Yoshikazu, K. Takahiro, M. Yasushi, T. Hitoshi, W. Makoto, H. Katsumi, Sugar micro needles as transdermic drug delivery system. *Biomed. Microdevices*, 7, 185–188 (2005).

[52] R.L. Bronaugh, R.F. Stewart, E.R Congdon. Methods for *in vitro* percutaneous absorption studies. II. Animal models for human skin. *Toxicol. Appl. Pharmacol.*, 62, 481–488 (1982).

[53] B. Godin, E. Touitou. Transdermal skin delivery: predictions for humans from *in vivo*, *ex vivo* and animal models. *Adv. Drug Deliv. Rev.*, 59, 1152–1161 (2007).

[54] C. Duquesnoy, J.P. Mamet, D. Sumner, E. Fuseau. Comparative clinical pharmacokinetics of single doses of sumatriptan following subcutaneous, oral, rectal and intranasal administration. *Eur. J. Pharm. Sci.*, 6, 99–104 (1998).

[55] B. Mazières, S. Rouanet, J. Velicy, C. Scarsi, V. Reiner. Topical ketoprofen patch (100 mg) for the treatment of ankle sprain: a randomized, double-blind, placebo-controlled study. *Am. J. Sports Med.*, 33, 515–523 (2005).

[56] A. Herwadkar, V. Sachdeva, L.F. Taylor, H. Silver, A.K. Banga. Low frequency sonophoresis mediated transdermal and intradermal delivery of ketoprofen. *Int. J. Pharm.*, 423, 289–296 (2012).

[57] J. Levin, H. Maibach. The correlation between transepidermal water loss and percutaneous absorption: an overview. *J. Control. Release*, 103, 291–299 (2005).

[58] J. Fokuhl, C.C. Müller-Goymann. Modified TWEL *in vitro* measurements on transdermal patches with different additives with regards to water vapour permeability kinetics. *Int. J. Pharm.*, 444, 89–95 (2013).

[59] N. Kanikkannan, R. Patel, T. Jackson, M.S. Shaik, M. Singh. Percutaneous absorption and skin irritation of JP-8 (jet fuel). *Toxicology*, 161, 1–11 (2001).

[60] T.R. Smith, J. Goldstein, R. Singer, N. Pugach, S. Silberstein, M.W. Pierce. Twelve-month tolerability and efficacy study of NP101, the sumatriptan iontophoretic transdermal system. *Headache*, 52, 612–624 (2012).

[61] M. Vikelis, D.D. Mitsikostas, A.M. Rapoport. Sumatriptan transdermal iontophoretic patch (NP101-Zelrix^{TM}): review of pharmacology, clinical efficacy, and safety in the acute of treatment of migraine. Neuropsychiatr. *Dis. Treat.*, 8, 429–434 (2012).

[62] H. Sevelius, R. Runkel, E. Segre, S.S. Bloomfield. Bioavailability of naproxen sodium and its relationship to clinical analgesic effects. *Br. J. Clin. Pharmacol.*, 10, 259–263 (1980).

[63] J.H. Draize, G. Woodard, H.O. Calvery. Methods for the study of irritation and toxicity of substances applied topically to the skin and mucous membranes. *J. Pharmacol. Exp. Ther.*, 82, 377–390 (1944).

[64] S. Liu, M.N. Jin, Y.S. Quan, F. Kamiyama, K. Kusamori, H. Katsumi, T. Sakane, A. Yamamoto. Transdermal delivery of relatively high molecular weight drugs using novel self-dissolving microneedle arrays fabricated from hyaluronic acid and their characteristics and safety after application to the skin. *Eur. J. Pharm. Biopharm.*, 86, 267–276 (2014).

[65] C.M. Dixon, D.A. Saynor, P.D. Andrew, J. Oxford, A. Bradbury, M.H. Tarbit. Disposition of sumatriptan in laboratory animals and humans. *Drug Metab. Dispos.*, 21, 761–769 (1993).

[66] J.H. Oh, H.H. Park, K.Y. Do, M. Han, D.H. Hyun, C.G. Kim, C.H. Kim, S.S. Lee, S.J.

Hwang, S.C. Shin, C.W. Cho. Influence of the delivery systems using a microneedle array on the permeation of a hydrophilic molecule, calcein. *Eur. J. Pharm. Biopharm.*, 69, 1040–1045 (2008).

[67] D. Huang, E.A. Swanson, C.P. Lin, J.S. Schuman, W.G. Stinson, W. Chang, M.R. Hee, T. Flotte, K. Gregory, C.A. Puliafito. Optical coherence tomography. *Science*, 254, 1178–1181 (1991).

[68] S. Marschall, B. Sander, M. Mogensen, T.M. Jørgensen, P.E. Andersen. Optical coherence tomography–current technology and applications in clinical and biomedical research. *Anal. Bioanal. Chem.*, 400, 2699–2720 (2011).

[69] R.F. Donnelly, M.J. Garland, D.I.J. Morrow, K. Migalska, T.R.R. Singh, R. Majithiya, A.D. Woolfson. Optical coherence tomography is a valuable tool in the study of the effects of microneedle geometry on skin penetration characteristics and in-skin dissolution. *J. Control. Release,* 147, 333–341 (2010).

[70] M.J. Garland, K. Migalska, T.M. Tuan-Mahmood, T.R.R. Singh, R. Majithija, E. Caffarel-Salvador, C.M. McCrudden, H.O. McCarthy, A.D. Woolfson, R.F. Donnelly. Influence of skin model on *in vitro* performance of drug-loaded soluble microneedle arrays. *Int. J. Pharm.*, 434, 80–89 (2012).

[71] S.M. Bal, J. Gaussin, S. Pavel, J.A. Bouwstra, *In vivo* assessment of safety of microneedle arrays in human skin, *Eur. J. Parm. Sci.*, 35, 193–202 (2008).

[72] D. Mohammed, K. Hirata, J. Hadgraft, M.E. Lane, Influence of skin penetration enhancers on skin barrier function and skin protease activity. *Eur. J. Parm. Sci.*, 51, 118–122 (2014).

[73] T. Jui-Chen, N.D. Weiner, G.L. Flynn, J. Ferry. Properties of adhesive tapes used for stratum corneum stripping. *Int. J. Pharm.*, 72, 227–231 (1991).

[74] C.P. Zhou, Y.L. Liu, H.L. Wang, P.X. Zhang, J.L. Zhang. Transdermal delivery of insulin using microneedle rollers *in vivo*. *Int. J. Pharm.*, 392, 127–133 (2010).

[75] A. Femenía-Font, C. Balaguer-Fernández, V. Merino, A. López-Castellano. Iontophoretic transdermal delivery of sumatriptan: effect of current density and ionic strength. *J. Pharm. Sci.*, 94, 2183–2186 (2005).

[76] V. Agrawal, V. Gupta, S. Ramteke, P. Trivedi. Preparation and evaluation of tubular micelles of pluronic lecithin organogel for transdermal delivery of sumatriptan. *AAPS PharmSciTech.*, 11, 1718–1725 (2010).

PUBLISHED PAPERS

1) Dan Wu, Yutaro Tanaka, Yong-ri Jin, Kunio Yoneto, Tammam Alama, Ying-shu Quan, Fumio Kamiyama, Kosuke Kusamori, Hidemasa Katsumi, Toshiyasu Sakane, Akira Yamamoto: Development of a novel transdermal patch containing sumatriptan succinate for the treatment of migraine: *in vitro* and *in vivo* characterization. *Journal of Drug Delivery Science and Technology*, 24, 695–701 (2014). [Chapter 1]

2) Dan Wu, Ying-shu Quan, Fumio Kamiyama, Kosuke Kusamori, Hidemasa Katsumi, Toshiyasu Sakane, Akira Yamamoto: Improvement of Transdermal Delivery of Sumatriptan Succinate Using a Novel Self-dissolving Microneedle Array Fabricated from Sodium Hyaluronate in Rats. *Biological and Pharmaceutical Bulletin*, 38, 365–373 (2015). [Chapter 2]